**Title:**

# Small RNA-mediated genomic silencing promotes telomere stability in the absence of telomerase

**Authors:**

Charlie Longtine[1,2,#], Stephen Frenk[1,2,#], Evan Lister-Shimauchi[1,2], and Shawn Ahmed[1,2,3]*

**Affiliations:**

[1]Department of Genetics, [2]Department of Biology, [3]Lineberger Comprehensive Cancer Center, University of North Carolina, Chapel Hill, NC, USA

# Equal contributions
*Correspondence and Lead Contact: shawn@med.unc.edu

Short title: small RNAs promote telomere stability

**Abstract**

Small RNAs with perfect homology to telomeres are exceptionally rare and their biological significance is unclear. We define an endogenous small RNA pathway in *Caenorhabditis elegans* that protects telomeres via Dicer, the perinuclear Argonaute protein WAGO-1, the nuclear Argonaute protein HRDE-1, and the HP1 protein HPL-2 that stabilizes H3K9me2. Loss of telomerase induces biogenesis of subtelomeric small RNAs, whereas loss of both telomerase and small RNA-mediated silencing induces expression of the telomeric lncRNA TERRA, DNA damage, and accelerated sterility. These phenotypes were rescued by exogenous telomeric small RNAs and by loss of the DNA damage response protein EXO-1. We propose that small RNA-mediated heterochromatin formation and telomerase function redundantly to repress a form of telomeric DNA damage that induces TERRA expression and could represent the natural substrate of telomerase. In conclusion, very rare small RNAs promote telomere stability, a concept that could be relevant to other segments of the genome.

## Introduction

Telomeres are repetitive nucleoprotein structures that protect the ends of linear eukaryotic chromosomes from degradation and recognition as double-stranded DNA breaks (Maciejowski and de Lange, 2017, Shay, 2016). Deficiency for telomerase reverse transcriptase in most human somatic cells results in progressive telomere erosion over cell divisions, which eventually triggers replicative senescence (Holohan et al., 2014, Shay, 2016). Telomere shortening thus acts as a barrier to tumorigenesis, but may also contribute to organismal aging through impaired stem cell function, regeneration, and organ maintenance (Donate and Blasco, 2011, Shay, 2016). Regulating the rate of telomere erosion in telomerase-negative cells is therefore crucial for maintaining the balance between tumor suppression and age-related tissue decline (Li et al., 2017, Maciejowski and de Lange, 2017). Tumor cells escape telomeretriggered senescence by stabilizing telomere length, either through reactivation of telomerase or through activation of the telomerase-independent recombination-

mediated telomere maintenance pathway termed Alternative Lengthening of Telomeres (ALT) (Pickett and Reddel, 2015).

Telomeres have features characteristic of heterochromatin in that they associate with the heterochromatin protein HP1 and contain transcriptionally repressive histone marks such as methylation of H3K9 and H4K20 (Benetti et al., 2007, McMurchy et al., 2017). Nonetheless, telomeres are transcribed into the G-rich long noncoding RNA (lncRNA) termed TERRA, a feature widely conserved among eukaryotes, and lower levels of the C-rich antisense lncRNA ARRET have also been reported (Azzalin et al., 2007). TERRA is transcribed from the subtelomere into the telomere by RNA polymerase II and is upregulated at shortened and damaged telomeres, where it may recruit telomerase and chromatin modifiers to promote telomere elongation (Azzalin and Lingner, 2015, Cusanelli et al., 2013). Telomere elongation represses expression of TERRA through increased heterochromatin marks at telomeres such as histone H3K9 methylation and HP1 binding (Arnoult et al., 2012). In contrast, shortened telomeres of mice deficient for telomerase or of mouse cells that overexpress the telomere-binding protein TRF2 display loss of heterochromatic marks at telomeres and subtelomeres (Benetti et al., 2007, Benetti et al., 2008). Telomere length has therefore been inversely correlated with TERRA expression and the heterochromatic state of telomeres, and TERRA expression in mouse cells has recently been linked to H3K9me3 and other heterochromatic histone marks present at mammalian telomeres (Montero et al., 2018).

Transcriptional silencing and heterochromatin deposition at repetitive segments of the genome such as the pericentromere require long non-coding RNA (lncRNA) transcripts that promote biogenesis of and interact with small RNAs (sRNAs) that direct heterochromatin factors to target these genomic loci (Holoch and Moazed, 2015, Reinhart and Bartel, 2002). Endogenous sources of double-stranded RNA such as sense-antisense transcript hybrids can be processed into small RNAs that play roles in creating and maintaining sRNA-mediated heterochromatin. In this context, RNA expression is paradoxically required for genomic silencing (Holoch and Moazed, 2015). Bidirectional transcription of telomeres has been linked to production of telomeric

101 sRNAs that are associated with the presence of subtelomeric DNA methylation in
102 *Arabidopsis* (Vrbsky et al., 2010). Similar telomeric sRNAs have also been observed in
103 *Tetrahymena*, mouse stem cells, and human cell lines (Cao et al., 2009, Couvillion et
104 al., 2009, Rossiello et al., 2017), and can promote the DNA damage response at
105 uncapped telomeres in mammals (Cao et al., 2009, Couvillion et al., 2009, Rossiello et
106 al., 2017). However, their functional relevance at canonical telomeres and their
107 interaction with telomerase is not well understood in any experimental system.
108
109 Germline transcription in *C. elegans* is regulated in part by a network of small RNA
110 pathways that promote silencing or expression of target loci in a sequence-specific
111 manner (Billi et al., 2014). Primary sRNA classes trigger production of secondary
112 sRNAs that can promote transcriptional silencing or mRNA destruction. One class of
113 primary sRNAs are 21 nucleotide Piwi-Interacting RNAs (piRNAs) that are created from
114 thousands of tiny genes that repress expression of potentially harmful foreign genetic
115 elements including transposons and transgenes (Batista et al., 2008, Das et al., 2008,
116 Kasper et al., 2014). piRNAs interact with PRG-1, a member of the Piwi clade of
117 Argonaute proteins, which can recognize piRNA targets based on sequence
118 complimentarity with up to 3 mismatches (Bagijn et al., 2012). RNA target recognition
119 triggers the recruitment of RNA-dependent RNA polymerases (RdRPs) that act in
120 Mutator bodies, which are associated with perinuclear P granules, to create *de novo* 22
121 nucleotide secondary sRNAs with a 5' guanine (22G RNAs) (Pak and Fire, 2007).
122 These 22G RNAs are loaded onto worm-specific Argonaute proteins (WAGOs) such as
123 the nuclear WAGO HRDE-1, which promotes heterochromatin deposition at target loci
124 (Ashe et al., 2012, Buckley et al., 2012). Germline transcription is protected by a
125 separate set of 22G RNAs that interact with the anti-silencing Argonaute protein CSR-1
126 (Avgousti et al., 2012, Wedeles et al., 2013). Aside from the piRNA pathway, 22G RNAs
127 can be created in response to primary sRNAs derived from other sources. For example,
128 DCR-1, the *C. elegans* homologue of the highly conserved RNAse class III enzyme
129 Dicer, can cleave endogenous double stranded RNA to create primary 26G RNAs,
130 which bind distinct Argonaute proteins to trigger RDRP-dependent silencing through the

22G RNA pathway described above (Bernstein et al., 2001, Ketting et al., 2001, Knight and Bass, 2001).

Here we describe an endogenous sRNA and heterochromatin pathway that functions redundantly with telomerase to repress TERRA and promote telomere stability.

## Results

### Loss of endogenous sRNAs or XNP-1/ATRX does not promote ALT

High levels of TERRA and loss of the histone H3.3 chaperone subunits ATRX and DAXX commonly occur in human ALT cancers (Flynn et al., 2015, Lovejoy et al., 2012). The ATRX/DAXX complex mediates histone H3.3 incorporation at telomeres and interacts with methylated H3K9 and HP1 to promote heterochromatin formation (Wong et al., 2010), which has been proposed to repress ALT by protecting telomeres from replication stress and TERRA expression (Udugama et al., 2015). We have previously shown that 10-20% of *C. elegans* strains that are deficient for telomerase can be maintained indefinitely through the activation of ALT (Cheng et al., 2012). Because human ALT cancers are characterized by ATRX-mediated heterochromatin dysfunction, we reasoned that small RNA factors that promote heterochromatin silencing might regulate the establishment of ALT. We tested this hypothesis by passaging *trt-1* telomerase mutant strains that were deficient for biogenesis of either primary or secondary sRNAs by transferring hundreds of worms per strain weekly, which reliably allows survival of 10-20% of strains via ALT (Cheng et al., 2012). Loss of either primary sRNAs (*trt-1; dcr-1)* or downstream secondary sRNAs (*trt-1; mut-7* and *trt-1; mut-14)* did not significantly alter the proportion of strains that survive via ALT (Figure 1A, Table S1). Similarly, loss of the histone H3.3 chaperone XNP-1/ATRX itself did not affect the establishment or maintenance of ALT (Table S1), indicating that loss of neither sRNA- nor XNP-1/ATRX-mediated heterochromatin formation is sufficient to promote ALT.

160 **Small RNA and heterochromatin factors repress rapid sterility when telomerase is**
161 **deficient**

162 *C. elegans trt-1* telomerase mutant strains do not remain fertile via ALT when 6 worms
163 are passaged weekly. Instead, when 20-40 strains per genotype are passaged, they
164 become uniformly sterile after growth for 20-30 generations in response to telomere
165 erosion (Ahmed and Hodgkin, 2000, Cheng et al., 2012, Meier et al., 2006). The sterility
166 of late-generation *trt-1* mutants is induced by a chromosome fusion and genome
167 catastrophe phenotype that is analogous to crisis observed in checkpoint-deficient
168 telomerase-negative mammalian cells. Intriguingly, *trt-1* mutant lines lacking primary or
169 secondary sRNA biogenesis factors became sterile significantly faster than *trt-1* single
170 mutants when they were passaged by transferring 6 L1 larvae per week (Figure 1B,
171 Table S2). sRNA-deficient *trt-1* mutant strains rapidly accumulated end-to-end
172 chromosome fusions by generation F12, a characteristic of telomerase mutants that
173 have grown for more than 20 generations (Figure 1G). *C. elegans* chromosome fusions
174 cause non-disjunction events during meiosis that elicit dominant embryonic lethality or
175 X0 male phenotypes in progeny of heterozygous F1 animals. We asked if
176 earlygeneration *trt-1; dcr-1* mutant animals possessed chromosome fusions by
177 performing genetic crosses that would be capable of revealing a single heterozygous
178 end-to-end chromosome fusion (Ahmed and Hodgkin, 2000). We crossed four
179 independently derived *trt-1 dcr-1* F4 hermaphrodites with N2 wild-type males but failed
180 to detect fused chromosomes that were present in generation F24 *trt-1* mutant controls
181 ($p = 3.841e-05$ for males and $p = 3.61e-05$ for dead embryos, Mann Whitney U test)
182 (Table S3). However, early-generation *trt-1; dcr-1* mutant strains displayed high levels of
183 DNA damage that were not observed for *trt-1* single mutant controls (Figure 1H).
184 Together, these results suggest that loss of small RNAs and telomerase elicits telomere
185 damage but not telomere fusions in early generations, and that the rapid sterility of
186 these strains in later generations is promoted by critically shortened telomeres that give
187 rise to abundant end-to-end chromosome fusions.
188
189 We created a number of sRNA-deficient *trt-1* double mutants to define additional small
190 RNA factors that promote telomere stability in the absence of telomerase. The telomeric

siRNA pathway included RDE-4, which binds endogenous dsRNA and forms a complex with the Dicer nuclease DCR-1, and the Argonaute RDE-1, which acts with the RNAdependent RNA polymerase RRF-3 to promote production of dsRNA-derived primary sRNAs (Gent et al., 2010, Steiner et al., 2009, Tabara et al., 2002) (Figure 1B). The MUTATOR proteins MUT-7 and MUT-14, which promote amplification of 22G secondary sRNAs that can promote transcriptional silencing in the nucleus (Billi et al., 2014, Ketting et al., 1999, Tijsterman et al., 2002), were also required to prevent rapid sterility in *trt-1* mutants (Figure 1B). Two other small RNA factors, RRF-2 and ERI-1, did not affect *trt-1* mutant sterility (Figure 1B), indicating that the endogenous 26G sRNA pathway that requires ERI-1 (Gent et al., 2010, Han et al., 2009) is dispensable for telomere stability in the absence of telomerase.

We crossed *dcr-1* and *mut-7* single mutants with wild-type males, singled F2 progeny that were homozygous mutant for *dcr-1* or *mut-7*, and isolated genomic DNA from F4, F6 and F8 generation descendants. Southern blotting revealed discrete telomere bands that display modest telomere erosion for freshly homozygous *dcr-1* and *mut-7* mutant telomeres (Figure S1A, B), although none of the small RNA single mutants we tested became progressively sterile or accumulated chromosome fusions (Figure 1G). We asked if the accelerated sterility of small RNA-deficient *trt-1* mutant strains might be explained by short telomeres inherited from gametes derived from small RNA-deficient grandparents using genetics, by crossing a *trt-1; dcr-1* double mutant hermaphrodite with *dcr-1* mutant males, singling *trt-1 +/-; dcr-1 -/-* F1 hermaphrodites and isolating *trt1; dcr-1* double mutant F2. This cross was repeated 15 times to create a *trt-1; dcr-1* double mutant strain whose telomeres should be exclusively derived from the *dcr-1* mutant background. The *trt-1; dcr-1* 15x strain became sterile slightly slower than freshly created *trt-1; dcr-1* double mutants, although this difference was not statistically significant ($p = 0.07$) (Figure 1F). These results indicate that shortened telomeres transmitted from the *dcr-1* mutant cannot explain the rapid sterility of *trt-1; dcr-1* double mutants. We analyzed the dynamics of telomere erosion in sRNA-deficient *trt-1* mutant strains using terminal restriction fragment analysis but did not observe a significant difference in the rate of telomere erosion when passaging multiple worms per plate, in

222 comparison to *trt-1* single mutant controls (p > 0.7 in both cases) (Figure S1A, B).
223 However, when we passaged individual worms for each genotype, we observed
224 significant levels of telomere instability in sRNA-deficient *trt-1* mutant strains in
225 comparison to *trt-1* single mutant controls. *trt-1; mut-7* and *trt-1; dcr-1* mutants had a
226 significantly larger variance in the rate of telomere erosion than *trt-1* mutants, which
227 resulted from atypical shortening and elongation events (Figure S2A, B).
228
229 We hypothesized that small RNAs might repress rapid sterility by directing chromatin
230 factors to telomeres to promote deposition of heterochromatic marks. *C. elegans*
231 telomeres have previously been reported to be enriched for H3K9me2 and bound by the
232 HP1 homolog HPL-2, which promotes H3K9me2 deposition and heterochromatin
233 formation, but not by the other *C. elegans* HP1 homolog HPL-1, which interacts with
234 H3K9me3 (Canzio et al., 2014, McMurchy et al., 2017). We confirmed that H3K9me2
235 but not H3K9me3 was enriched at *C. elegans* telomeres using high throughput
236 sequencing data sets generated from chromatin immunoprecipitation (ChIP)
237 experiments performed by independent groups (McMurchy et al., 2017, Zeller et al.,
238 2016). Moreover, we observed small H3K9me2 domains that extended into the
239 subtelomere at all *C. elegans* chromosome ends (Figure 3A-C). Similar to primary and
240 secondary sRNA-deficient *trt-1* strains, loss of HPL-2 but not HPL-1 caused accelerated
241 senescence in *trt-1* mutants (Figure 1C). H3K4 methylation, which is associated with
242 regions of active transcription, must be removed by demethylases prior to deposition of
243 repressive H3K9 methylation (Greer et al., 2010, Li et al., 2008), and we found that loss
244 of either of the two *C. elegans* H3K4 demethylases RBR-2/KDM5 or SPR-5/LSD1
245 caused rapid sterility of *trt-1* mutants (Figure 1C). Thus, H3K4 demethylation and
246 H3K9me2 deposition prevent telomere instability in the absence of telomerase.
247
248 The histone remodeling protein XNP-1/ATRX has previously been implicated in
249 telomeric heterochromatin formation and interacts with unmethylated H3K4 and
250 methylated H3K9 deposited on the histone variant H3.3 (Udugama et al., 2015). *trt-1*
251 *xnp-1* double mutants became sterile significantly faster than *trt-1* single mutants but not
252 as fast as small RNA deficient *trt-1; mut-7* double mutants (Figure 1D). This suggests

253 that XNP-1 may mediate some, but not all, heterochromatin formation at telomeres,
254 possibly because sRNA-dependent methylation of histones other than H3.3, such as
255 canonical histone H3, can promote telomere stability. Additionally, as loss of both *xnp-1*
256 and *mut-7* did not exacerbate the accelerated sterility phenotype of sRNA-deficient *trt-1*
257 mutant strains (Figure 1D), these genes function in the same telomere stability pathway.
258 These data suggest that the chromatin remodeler XNP-1/ATRX may act in germ cells to
259 promote heterochromatin formation at telomeres in response to sRNAs.
260
261 **Increased expression of TERRA in small RNA and chromatin deficient *trt-1* strains**
262 We hypothesized that DCR-1 and RDE-4 may interact with telomeric dsRNA produced
263 from bidirectional transcription of telomeres into TERRA and ARRET to create primary
264 sRNAs that are then amplified into a secondary sRNA population that triggers small
265 RNA-dependent silencing of TERRA (Rossiello et al., 2017, Vrbsky et al., 2010). To test
266 whether small RNA and chromatin factors regulate telomeric transcription we measured
267 the abundance of TERRA by qRT-PCR at three chromosome ends using primers within
268 their H3K9me2-coated subtelomere domains (Figure 3A-C). Compared to *trt-1* single
269 mutant controls, TERRA was upregulated in early-generations in three strains - *trt-1;*
270 *rde-4* and *trt-1; mut-14* and *trt-1; spr-5* double mutants - but not in *trt-1* or sRNA-
271 deficient single mutant controls (Figure 2A). These results are distinct from previous
272 observations that show that TERRA transcription can be specifically induced at
273 damaged or shortened telomeres of mammalian cells that possess telomerase (Porro et
274 al., 2014, Rossiello et al., 2017).
275
276 We next used RNA Fluorescence *In Situ* Hybridization (FISH) to confirm the effects on
277 TERRA expression and to examine its cell and tissue localization. In wild-type control
278 and *trt-1* mutant hermaphrodite and male worms, TERRA was expressed at low levels
279 in the soma as well as in the pachytene region of the meiotic germline (Figures 2B-D,
280 S3-4), which corresponds to the location of several lncRNA-mediated germline silencing
281 processes (Taylor et al., 2015), including Meiotic Silencing of Sex Chromosomes in
282 mammals and *C. elegans* (Heard and Turner, 2011) and a transcriptional burst of
283 piRNAs in mammals that primes genomic silencing in germ cells prior to gametogenesis

284 (Gou et al., 2014). Compared to both wild-type control and *trt-1* or *dcr-1* single mutant
285 strains, *trt-1; dcr-1* double mutant strains had increased expression of TERRA in the
286 germline (Figures 2B-D, S3) and soma (Figures S3-4) by the F6 generation. We
287 observed an increase in the number of TERRA foci per nucleus in sRNA-deficient *trt-1*
288 mutants, which are likely to occur at telomeres (Figure 2D), although this remains to be
289 formally demonstrated. We also observed TERRA expression by RNA FISH in the
290 cytoplasm and nucleoplasm of sRNA-deficient *trt-1* cells (Figure 2B-C, S3), which might
291 be consistent with possible non-telomeric functions of TERRA (Chu et al., 2017, Roake
292 and Artandi, 2017) or with a role for TERRA in protecting telomeres *in trans* (Montero et
293 al., 2018). This suggests that endogenous sRNAs may repress telomeric transcription
294 in the absence of telomerase, although it is also possible that subtelomeric transcription
295 may be a consequence of the telomere state that occurs in sRNA-deficient telomerase
296 mutants, which experience high levels of DNA damage signaling (Figure 1H).
297
298 **Subtelomeric sRNAs are upregulated in telomerase mutants**
299 Telomeric sRNAs have been observed in protists, plants, and mammals (Cao et al.,
300 2009, Couvillion et al., 2009, Vrbsky et al., 2010). We recently interrogated 92 publicly
301 available small RNA sequencing libraries created from RNA isolated from various *C.*
302 *elegans* strains and found rare reads that mapped perfectly to the *C. elegans* telomere
303 repeat $(TTAGGC)_n$, occurring at a frequency of 1 per 10,000,000 reads (Frenk et al.,
304 2019). piRNAs with up to 3 mismatches can target regions of the *C. elegans* genome for
305 silencing (Bagijn et al., 2012), and we found that telomeric sRNAs with up to 3
306 mismatches were substantially more abundant than those with perfect telomere repeat
307 sequence (1 per 100,000) (Frenk et al., 2019). We compared levels of telomeric sRNAs
308 with mismatches from wildtype with those of mutants for small RNA genes that promote
309 telomere stability in the absence of telomerase, such as *dcr-1*, *rde-4*, *mut-7*, and *mut14*,
310 and found that levels of telomeric sRNAs were sometimes depleted in these
311 backgrounds, but not always (File S1).
312
313 We asked if loss of telomerase might alter levels of telomeric sRNAs in a manner that
314 might depend on Dicer by isolating RNA from wild-type control, *trt-1* single mutant, and

315 *trt-1; dcr-1* double mutant strains and preparing small RNA libraries. We sequenced
316 these libraries deeply in an effort to detect rare perfect telomeric sRNAs. We obtained
317 ~20,000,000 reads each for 6 data sets and found that our *trt-1; dcr-1* data sets were
318 strongly depleted of 22G RNAs that were previously reported to depend on *dcr-1*
319 (Figure S5A) (Gent et al., 2010). To assess TRT-1-dependent changes in sRNAs
320 throughout the genome, we counted the number of 22G reads mapping uniquely
321 antisense to protein-coding genes and found upregulation of sRNAs at 720 loci and
322 downregulation at 456 loci in *trt-1* animals compared with wild-type controls (Figure
323 S5B). Of the upregulated loci, 465 were not upregulated in *trt-1; dcr-1* animals
324 compared with wildtype, indicating DCR-1 dependence. We did not find significant GO
325 terms in loci with either up or downregulated sRNA production. Given that *trt-1* is
326 expressed at high levels in *C. elegans* germ cells (Meier et al., 2006), we asked whether
327 the loci with differential sRNA production were enriched for germline-enriched genes.
328 We used previously published data on germline expression (Ortiz et al., 2014) and
329 found significant enrichment for germline-enriched genes in both upregulated and
330 downregulated loci ($p < 1e-19$ and $p < 1e-33$ respectively, Pearson's Chi Square test
331 with Bonferroni correction) (Figure S5C). This may reflect an epigenetic response to
332 deficiency for telomerase in germ cells, even though early-generation *trt-1* mutants from
333 which the RNA was prepared had normal levels of fertility. sRNAs mapping to
334 transposons were unaffected by loss of TRT-1, with the exception of the CER-10 LTR
335 retrotransposon, for which sRNAs were three-fold downregulated (Figure S5D).
336
337 We found that levels of telomeric sRNAs with 1 to 3 mismatches did not change
338 substantially in sRNAs from *trt-1* single mutants or *trt-1; dcr-1* double mutants, but
339 detected no sRNAs composed of perfect telomere repeats in any genetic background
340 (Figure 4A). We next examined 22G RNAs at subtelomeric regions (defined as 2kb of
341 sequence adjacent to each telomere) and found that these were present in wild-type
342 samples at the left end of chromosome *III*, and that their abundance was increased
343 twofold in *trt-1* single mutants and their presence almost entirely eliminated in *trt-1; dcr-*
344 *1* double mutants (Figure 4C, E). Subtelomeric sRNAs were also observed within 1kb of
345 the telomere at the left ends of chromosomes *I* and *IV* in *trt-1* mutants and not in

346 wildtype or *trt-1; dcr-1* double mutants (Figure 4B, D). The right ends of Chromosomes *I*
347 and *III* and the left end of Chromosome *II* all showed at least a two-fold increase in
348 subtelomeric sRNAs in *trt-1* and/or *trt-1; dcr-1* double mutants (Figure 4E). We observed
349 a significant bias for subtelomeric sRNAs whose sequences correspond to the C-rich
350 telomere strand (antisense to TERRA) for the left ends of Chromosomes *I* and *III* ($p <$
351 $1e-13$ and $p < 1e-43$ respectively, binomial test with Bonferroni correction) and for the
352 right arm of Chromosome *I* ($p < 1e-172$, binomial test with Bonferroni correction) while
353 the nucleotide sequences of subtelomeric sRNAs at the left arm of Chromosome *IV* and
354 the right arm of Chromosome *III* showed a bias for subtelomeric TERRA, suggesting
355 that they were created from ARRET ($p < 1e-11$, $p = 0.006$ respectively, binomial test
356 with Bonferroni correction) (Figure 4F). These observations suggest that telomere
357 dysfunction triggers the upregulation of small RNA biogenesis at multiple subtelomeres
358 through both DCR-1-dependent and -independent mechanisms. sRNA biogenesis might
359 be induced at a subset of subtelomeres when telomerase is dysfunctional because 1)
360 shortened telomeres inherited from *trt-1* mutant gametes that created *trt-1* single
361 mutants might trigger sRNA biogenesis, or 2) DNA damage that occurs stochastically at
362 specific subtelomeres elicits sRNA biogenesis. Subtelomeric siRNAs that correspond to
363 the G- or C-rich telomeric strand at specific subtelomeres could be related to the
364 presence of transcripts that can be targeted for sRNA biogenesis at these telomeres.
365
366 We next interrogated data sets of small RNAs that immunoprecipitate with Argonaute
367 proteins that are known to promote silencing in the germline, HRDE-1 and WAGO-1, as
368 well as with the germline anti-silencing Argonaute CSR-1 (Gu et al., 2009, Claycomb et
369 al., 2009, Ashe et al., 2012). Enrichment of small RNAs for each protein was calculated
370 by dividing the number of reads in the immunoprecipitate library by the number of reads
371 in the corresponding input library. Telomeric sRNAs were enriched in WAGO-1
372 immunoprecipate relative to input, but this was not the case for HRDE-1 or CSR-1
373 (Figure 3D). Enrichment of subtelomeric small RNAs in WAGO-1 was detected at all
374 chromosome ends tested apart from the right arm of Chromosome *I* (some
375 chromosome ends were not tested due to an absence of reads in the input library).
376 Enrichment was also detected for HRDE-1 at all chromosome ends excluding the right

377 arm of Chromosome *I* and the left arm of Chromosome *III* (Figure 3E). Interestingly,
378 CSR-1 showed the opposite pattern of enrichment to WAGO-1 and HRDE-1, with
379 enrichment at none of the chromosome ends apart from the right end of Chromosome *I*.
380 The ribosomal DNA, the most highly expressed locus in the *C. elegans* genome, is
381 immediately adjacent to this telomere (Wicky et al., 1996), and it is therefore possible
382 that sRNA activity takes a predominantly anti-silencing function at this chromosome
383 end. We asked if either Argonaute that associates with telomeric or sub-telomeric
384 sRNAs, WAGO-1 or to a lesser degree HRDE-1, promotes telomere maintenance in the
385 absence of telomerase and found that *wago-1 trt-1* and *trt-1; hrde-1* double mutants
386 both displayed rapid sterility phenotypes in comparison to *trt-1* single mutants ($p < 1e11$
387 and $p < 1e-12$, respectively, log rank test) (Figure 1E).
388
389 **Telomeric sRNAs and loss of EXO-1 repress sterility in the absence of telomerase**
390 TERRA transcription in *S. pombe* initiates in the subtelomere but rarely extends into the
391 telomere (Moravec et al., 2016), so TERRA might serve as a template for
392 RDRPmediated biogenesis of subtelomeric sRNAs but might rarely yield perfect
393 telomeric sRNAs. It might be difficult to simultaneously target the 11 unique
394 subtelomeres of the *C. elegans* genome with exogenous subtelomeric sRNAs in an
395 effort to show that this class of sRNAs promotes telomere stability in the absence of
396 telomerase. Therefore, we decided to test the hypothesis that perfect telomere repeat
397 sRNAs can promote telomere stability in the absence of telomerase, even though we
398 failed to detect these rare sRNAs in our own sequencing experiments (Figure 4A). We
399 asked if introduction of exogenous telomeric sRNAs could rescue the rapid sterility of
400 sRNA-deficient *trt-1* mutants using a viable *dcr-1* allele, *mg375*, which is deficient for
401 endogenous sRNA production but is hypersensitive to exogenous RNAi when fed *E. coli*
402 expressing dsRNA (Welker et al., 2010). *trt-1; dcr-1(mg375)* double mutant strains that
403 were passaged on bacteria expressing telomeric dsRNA remained fertile significantly
404 longer than those expressing dsRNA from an empty vector control (Figure 4A). In
405 contrast, exogenous telomeric dsRNA did not affect the onset of sterility for *trt-1* single
406 mutant controls. Moreover, *trt-1; dcr-1(mg375)* strains fed telomeric dsRNA had
407 markedly reduced levels of DNA damage at F6 in comparison to *trt-1; dcr-1(mg375)*

408 strains grown on control RNAi or on regular OP50 bacteria that do not express dsRNA
409 (Figure 1F, 5C).
410
411 In budding yeast, artificially-induced TERRA overexpression promotes telomere
412 shortening *in cis* by forming RNA:DNA hybrids that stall telomeric replication forks in a
413 manner that stimulates telomere resection by the exonuclease Exo1 (Maicher et al.,
414 2012, Pfeiffer and Lingner, 2012). We therefore hypothesized that loss of EXO-1 might
415 rescue the accelerated sterility phenotype in sRNA-deficient telomerase mutants. *trt-1;*
416 *exo-1; mut-14* triple mutant lines survived significantly longer than *trt-1; mut-14* double
417 mutants (Figure 5B) and displayed reduced levels of DNA damage and moderate levels
418 of TERRA at generation F6 (Figures 5B, S5). Moreover, *trt-1; exo-1* double mutant
419 controls remained fertile even longer than *trt-1* single mutants (Figure 5B), indicating
420 that EXO-1-mediated telomere resection promotes telomere-shortening-induced
421 senescence in the absence of telomerase, both at normal telomeres and at telomeres
422 lacking sRNA-mediated genomic silencing. While *trt-1; exo-1* double mutant controls
423 remained fertile longer than *trt-1* single mutants, this was not true for *trt-1* single
424 mutants grown on exogenous telomeric dsRNA (Figure 5A, B). Thus, *exo-1* has at least
425 two roles at telomeres, one that promotes sterility when telomerase is absent and a
426 second that promotes sterility when telomerase and sRNA silencing is absent.
427
428
429 **Discussion**
430 Small RNAs promote genomic silencing of many types of transposons (Holoch and
431 Moazed, 2015), including those found at *Drosophila melanogaster* telomeres, which are
432 composed of non-LTR retrotransposons that are distinct from the simple repetitive
433 sequences that are maintained by telomerase and cap chromosome ends in most
434 organisms (Pardue and DeBaryshe, 2003). Components of the RNAi machinery
435 function at *Drosophila* telomeres to repress expression of HeT-A and TART
436 retrotransposons and their accumulation at chromosome termini (Pane et al., 2007,
437 Savitsky et al., 2006), even though they do not affect telomere capping (Perrini et al.,
438 2004). In contrast, loss of the *Drosophila* homologs of the heterochromatin-mediated

439 genome silencing proteins HP1 and ATRX causes immediate telomere deprotection and
440 fusion (Chavez et al., 2017, Fanti et al., 1998, Fulcher et al., 2014). H3K9me2 but not
441 H3K9me3 is present at wild-type *C. elegans* telomeres (Figure 3A-C) (McMurchy et al.,
442 2017, Zeller et al., 2016), and we found that the *C. elegans* HP1 homolog HPL-2 that
443 binds to and specifically stabilizes H3K9me2 (McMurchy et al., 2017) promotes
444 telomere stability in the absence of telomerase (Figure1C). We also identified factors
445 that create rare small RNAs that are likely to guide the deposition of histone silencing
446 marks in response to damaged telomeres (Figure 6A). Therefore, small RNAs and
447 heterochromatin proteins represent conserved features of both non-canonical and
448 canonical telomeres, even though their functions are distinct.
449
450 Loss of telomerase and sRNA factors in *C. elegans* caused high levels of DNA damage
451 response signaling in germ cells, but did not result in telomere fusions for a number of
452 generations, each generation representing 8-10 cell divisions. Therefore, the
453 accelerated sterility phenotype of sRNA-deficient *trt-1* mutants is not a consequence of
454 a defect in acute telomere uncapping, but rather an acceleration of the onset of crisis.
455 Biochemical analysis of telomere erosion in sRNA-deficient *trt-1* mutants revealed
456 increased variance in telomere size, which could be due to an error-prone
457 recombinational response to a form of DNA damage such as a stalled replication fork
458 (Figure 6C-D). Although both elongation and shortening of telomeres occurred (Figure
459 S1,S2), the shortening events are likely responsible for the premature end-to-end
460 chromosome fusion and sterility phenotypes of sRNA-deficient *trt-1* mutants. In
461 telomerase single mutants that are proficient for sRNA-mediated heterochromatin
462 deposition, telomeric DNA damage may be healed by a more precise DNA repair
463 pathway that more accurately maintains telomere length and is coupled to expression
464 and subsequent sRNA-mediated silencing of TERRA (Figure 6A-B).
465
466 Heterochromatin is known to suppress replication-based DNA damage at repetitive
467 segments of the genome (Zeller et al., 2016, Janssen et al., 2018). However, repeated
468 crossing of a *trt-1* mutation into a *dcr-1* mutant background failed to exacerbate the
469 accelerated sterility of *trt-1; dcr-1* double mutants (Figure 1F), indicating that

470 *dcr1(mg375)* mutants have telomeres of normal length. Therefore, telomerase-
471 mediated telomere repeat addition is likely to be an effective method of healing
472 telomeric DNA damage in the absence of sRNA-mediated heterochromatin deposition.
473 As telomerase activity in *C. elegans* requires proteins that respond to various forms of
474 DNA damage, such as the 9-1-1 sliding clamp (Ahmed and Hodgkin, 2000, Boerckel et
475 al., 2007, Meier et al., 2009), it is possible that the form of telomeric DNA damage that
476 compromises sRNA-deficient telomerase mutants occurs occasionally at wild-type
477 telomeres and represents the natural substrate for telomerase.
478
479 Loss of telomeric sRNA biogenesis in telomerase mutants resulted in TERRA
480 expression, which could create R-loops that induce homologous recombination in a
481 manner that creates telomere shortening events that are toxic (Figure 6C). As
482 exogenous telomeric sRNAs were sufficient to suppress telomere instability, DNA
483 damage signaling and TERRA expression in the absence of telomerase and
484 sRNAmediated heterochromatin formation (Figure 5), silencing of TERRA could be an
485 integral part of a telomeric DNA damage response (Figure 6B,D) (Toubiana and Selig,
486 2018). These results are consistent with a role for TERRA expression in the DNA
487 damage response at telomeres discussed by several recent studies. First, in mammals
488 TERRA expression can occur in response to a distinct form of telomeric damage that
489 occurs in the presence of telomerase – acutely deprotected, non-replicating telomeres–
490 and is accompanied by production of telomeric sRNAs that promote DNA damage
491 response factor recruitment (Rossiello et al., 2017). Second, a recent study in *S.*
492 *cerevisiae* showed that increased TERRA expression and persistent telomeric R-loops
493 in telomerase mutants can repress senescence by promoting recombination, indicating
494 that increased levels of TERRA are coupled to induction of a telomeric DNA damage
495 response (Graf et al., 2017). Third, elevated levels of TERRA have been shown to
496 contribute to senescence in *S. cerevisiae* (Wanat et al., 2018).
497
498 Reduced levels of TERRA and DNA damage signaling occurred in sRNA-deficient
499 telomerase mutants that lack *exo-1*. Consistently, loss of EXO1 in telomerase-negative
500 mice has been shown to extend lifespan and improve organ maintenance by repressing

501 telomeric ssDNA formation and DNA damage response (Schaetzlein et al., 2007),
502 suggesting a conserved role for EXO1 in the metazoan response to dysfunctional
503 telomeres. Expression of TERRA at mammalian telomeres induces EXO1-dependent
504 telomere shortening in a manner that independent of RNase H (Pfeiffer and Lingner,
505 2012). We did not test a role for RNase H in the telomere instability phenotype of
506 sRNA-deficient *C. elegans* telomerase mutants.
507
508 While this study was in progress, we found that *C. elegans* telomeric sRNAs with
509 mismatches could be mapped to Interstitial Telomere Sequences, which are degenerate
510 telomere tracts that are abundant on chromosomes arms and are distinct from
511 telomeres (Frenk et al., 2019). Interstitial Telomere Sequences were enriched in
512 introns, were often heterochromatic, and were depleted from 5' and 3' UTRs (Frenk et
513 al., 2019). As telomeric sRNAs with mismatches were not altered by the *dcr-1(mg375)*
514 mutation that causes telomere instability in the absence of telomerase (Figure 4A), we
515 suggest that they do not function at telomeres but instead promote transcriptional and
516 post-transcriptional gene silencing at non-telomeric segments of the genome.
517 Therefore, upregulated transcription of Interstitial Telomere Sequences that might cross-
518 hybridize with our RNA FISH telomere probe is unlikely to occur in *trt-1; dcr-1* mutants
519 that display high levels of TERRA (Figure 2).
520
521 Comparisons of sRNAs in three *Caenorhabditis* species revealed that although
522 telomeric sRNAs with mismatches contained a mixture of all four 5' nucleotides, sRNAs
523 composed of perfect telomere repeats were strongly depleted for 5' G nucleotides
524 (Frenk et al., 2019). The unique structural properties of perfect telomeric sRNAs
525 suggests a mechanism of biogenesis that is distinct from known classes of *C. elegans*
526 sRNAs (Billi et al., 2014). Although perfect telomeric sRNAs are very rare in published
527 data sets of *C. elegans* and mammals (Frenk et al., 2019), we found that perfect
528 telomeric sRNAs from the environment were sufficient to promote telomere stability in
529 *trt-1; dcr-1* mutants (Figure 5A). This suggests that very rare endogenous perfect
530 telomeric sRNAs promote genomic silencing of TERRA in the absence of telomerase,
531 which could prevent telomeric DNA damage (R-loops) or could promote DNA repair at

532 telomeres if expression and subsequent silencing of TERRA is coupled to the telomeric
533 DNA damage response (Figure 6). We conclude that very rare perfect telomeric small
534 RNAs, which might appear fleeting or artefactual based on analysis of RNA sequencing
535 data sets, promote telomere stability in the absence of telomerase. Similar classes of
536 rare small RNAs, which may be difficult (Frenk et al., 2019) or impossible (Figure 4A) to
537 measure, could be relevant to other segments of the genome.
538
539 As both Dicer and the dsRNA-binding protein RDE-4 promoted telomere stability in the
540 absence of telomerase (Figure 1B), we propose that biogenesis of telomeric small
541 RNAs initially involves transcription of G- and C-strands of the telomere, which creates
542 dsRNA molecules that are transported to perinuclear P granules (germ granules)
543 (Figure 6A). Telomeric dsRNA may then interact with RDE-4 and Dicer to create a
544 primary sRNA population that is amplified in adjacent Mutator bodies by RdRPs to
545 create 22G effector sRNAs (Figure 6A). We detected subtelomeric sRNAs that were
546 dependent on Dicer and that interacted with the Argonaute proteins WAGO-1 and
547 HRDE-1, both of which promoted telomere stability in the absence of telomerase.
548 These Argonaute proteins are known to act in germ cells to target overlapping groups of
549 transcripts, including genes, transposons, and pseudogenes (Gu et al., 2009). Although
550 WAGO-1 localizes to perinuclear P-granules (germ granules), where it might promote
551 either transcriptional or post-transcriptional gene silencing (Gu et al., 2009), HRDE-1
552 localizes to the nucleus where it promotes transcriptional gene silencing. Moreover,
553 HRDE-1 and WAGO-1 have been shown to function redundantly to promote a form of
554 permanent transgenerational transcriptional silencing (Ashe et al., 2012, Buckley et al.,
555 2012). Although proteomics has been performed for both HRDE-1 and WAGO-1, they
556 do not physically interact with one another or possess common interacting proteins
557 (Akay et al., 2017, Shirayama et al., 2014).
558
559 Although we were unable to measure perfect telomeric sRNAs by deeply sequencing
560 small RNAs from several genetic backgrounds (Figure 4A), we did observe upregulation
561 of sRNAs at some subtelomeres in telomerase mutants, and in some cases this
562 increase was DCR-1-dependent (Figure 4). We also found that HRDE-1 and WAGO-1

interact with 22G sRNAs that map to distinct and overlapping subtelomeres. Given that DNA damage responses induce histone modifications that can be propagated for long distances from sites of DNA damage (Polo and Jackson, 2011), we propose that the biological response to telomeric DNA damage initially involves very rare perfect telomeric sRNAs at chromosome termini. The telomeric DNA damage response may then spread such that more abundant sRNAs are created from RNA transcripts at some subtelomeric loci. Therefore, the variable sRNA biogenesis patterns observed at distinct subtelomeres of telomerase mutants may reflect a wider epigenetic consequence of the biological response to telomeric DNA damage.

In mammals, TERRA facilitates transcriptional regulation of the epigenome (Chu et al., 2017). Moreover, both TERRA and telomerase have been implicated in regulation of genes that promote stem cell proliferation (Marion et al., 2019, Sarin et al., 2005). Therefore, the interplay of telomerase and TERRA in the context of deficiency for small RNA-mediated genome silencing could reflect more general roles for these factors in epigenetic regulation of cell fate.

sRNA-mediated telomeric silencing was promoted by the *C. elegans* secondary sRNA biogenesis factor MUT-7 (Figure 1A, B), which is homologous to the exonuclease domain of human WRN1 Werner's syndrome protein whose loss results in early-onset aging of multiple tissues (Ketting et al., 2001). WRN1 deficiency is accompanied by accelerated telomere erosion and senescence phenotypes that can be rescued by telomerase expression (Shimamoto et al., 2015). While WRN1 and its homologs have been intensively studied for their roles in DNA recombination, WRN1 was recently shown to safeguard the stability of heterochromatin (Zhang et al., 2015), which our study suggests may play a critical role in maintenance of telomere stability in most human somatic cells. Consistently, deficiency for DNA methylation at repetitive segments of the genome, including telomeres, occurs in ICF syndrome cells that undergo rapid telomere shortening and senescence accompanied by increased TERRA expression, telomeric R-loops and DNA damage (Sagie et al., 2017). As global dysfunction of the epigenome is a hallmark of human aging (Zhang et al., 2015), our

594 findings may be generally relevant to understanding how sRNA-driven chromatin states
595 that are established in germ cells or the early embryo might contribute to telomere
596 instability during aging of adult somatic cells.
597
598
599 **Materials and Methods**
600
601 Strains: Unless otherwise noted, all strains were maintained at 20°C on nematode
602 growth medium plates seeded with *Escherichia coli* OP50. Strains used include Bristol
603 N2 ancestral, *wago-1(tm1414)*, *trt-1(ok410), unc-29(e193), dpy-5(e61), dcr-1(mg375),*
604 *hrde-1(tm1200), rde-1(ne219), rde-4(ne299), rrf-3(mg373), rrf-2(ok210), eri-1(mg366),*
605 *mut-7(pk204), mut-7(pk720), mut-14(pk738), rbr-2(tm1231), spr-5(by101),*
606 *xnp1(ok1823), xnp-1(tm678), hpl-1(tm1624), hpl-2(ok916), hpl-2(tm1479),* and
607 *exo1(tm1842)*. A *trt-1 unc-29* double mutant, where *unc-29* is tightly linked to *trt-1*, was
608 used to create strains used in this study. Double, triple, and quadruple mutants were
609 created using standard marker mutations and verified based on phenotype or genotype.
610 *mut-7* and *mut-14* mutants are known to accumulate transposon-induced mutations, so
611 these strains were outcrossed several times before use.

612 DAPI staining: One-day-old adults were washed twice in M9, soaked in 150 µL of
613 400ng/mL DAPI in ethanol solution for 30 min or until evaporated, rehydrated in 2 mL of
614 M9 solution overnight at 4°C, and mounted in 8 µL VECTASHIELD mounting medium
615 (Vector Laboratories). Chromosome counts were performed under 60x magnification
616 and a 359nm excitation wavelength using a Nikon Eclipse E800 microscope.

617 qPCR: Non-starved mixed-stage worms were washed with M9 and RNA was extracted
618 using 1 mL TRIZOL according to the manufacturer's instructions. For RT-PCR analysis,
619 total RNA was treated twice with DNase I and was reverse transcribed with primers for a
620 reference gene *act-1* and a telomere-specific primer $(GCCTAA)_3$ using SuperScript II
621 reverse transcriptase (Invitrogen). For SYBR green reactions, subtelomere specific
622 primers were designed within 200bp of the telomere-subtelomere junction.
623

624 RNA FISH: RNA FISH was performed as previously described (Sakaguchi et al., 2014)
625 with several modifications. In brief, non-starved, mixed-stage animals were washed
626 twice in M9 and three times in 1x DEPC-treated PBS. Worms were fixed in 1mL fixation
627 buffer (1x DEPC-treated PBS with 3.7% formaldehyde) for 45 min rotating at room
628 temperature then washed twice in 1mL 1x DEPC-treated PBS. Fixed animals were
629 permeabilized overnight at 4°C in 70% ethanol in DEPC-treated $H_2O$, then washed in 1
630 mL wash buffer [10% (vol/vol) formamide in 2x RNases-free SSC]. Aliquots of each
631 sample were removed prior to hybridization and treated with RNaseA for 1h at 37°C to
632 ensure probe specificity to RNA. Hybridization was performed at 30°C overnight in 100
633 µL hybridization buffer (10% dextran sulfate, 2x RNase-free SSC, 10% deionized
634 formamide, 0.02% RNase-free BSA, 50 µg *E. coli* tRNA) with 1.25 µM probe.
635 Cy5labelled $(GCCTAA)_3$ probe was used to detect TERRA transcripts. Animals were
636 washed twice with wash buffer, counterstained with 25 ng/mL DAPI for 30 min at room
637 temperature, and mounted on glass slides in VECTASHIELD mounting medium (Vector
638 Laboratories) before epifluorescence microscopy.
639
640 IF: IF was carried out as previously described (Phillips et al., 2009) by fixing dissected
641 gonads of 1 day old adults in 2% PFA for 10 minutes followed by a 1 minute postfixation
642 in methanol. Rabbit anti-pS/TQ (Cell Signaling Technology) was used at a 1:500 dilution
643 and mouse anti-RNA:DNA hybrid S9.6 at 1:500 dilution. Stained gonads were
644 counterstained with DAPI and mounted with VECTASHIELD (Vector laboratories) before
645 epifluorescence microscopy.
646
647 RNAi: RNAi clone expressing dsRNA targeting *C. elegans* telomeres was constructed
648 using NEB HiFi DNA assembly mix according to the manufacturer's instructions. 200 bp
649 of telomeric repeats were amplified from cTel55x by PCR with 20 bp overlap to SpeI
650 digested L4440. Correct constructs were transformed into HT115 and RNAi was
651 performed as previously described (McMurchy et al., 2017).
652
653 Southern Blot: *C. elegans* genomic DNA was digested overnight with Hinf1 (New

654 England Biolabs), separated on a 0.8% agarose gel at 1.5 V/cm, and transferred to a
655 neutral nylon membrane (Hybond-N, GE Healthcare Life Sciences). A
656 digoxigeninlabelled telomere probe was hybridized and detected as described
657 (Ahmed and Hodgkin, 2000). Migration distance was measured using ImageJ.
658
659 Mrt and ALT assays: When telomerase-deficient *trt-1(ok410) C. elegans* mutants are
660 passaged by using the standard Mortal Germline (Mrt) assay developed in our
661 laboratory, which involves passaging six L1 larval animals to fresh plates weekly, 100%
662 become sterile within 20–30 generations. When *trt-1(ok410)* strains are passaged
663 weekly by transferring a 1cm$^2$ chunk of agar populated with ≈200–400 animals, 10-20%
664 of the strains survive for hundreds of generations. Mantel-Cox Log Rank Analysis was
665 used to determine differences of transgenerational lifespan between strains. A z-test
666 was performed to compare proportion of ALT survivors in chunked strains.
667
668 RNA-seq: Animals were grown at 20°C on 100 mm NGM plates seeded with OP50
669 bacteria. Two biological replicates were prepared for each genotype. RNA was
670 extracted using Trizol (Ambion) followed by isopropanol precipitation. RNA samples
671 were treated with 20U RNA 5' polyphosphatase (Lucigen, RP8092H) for 30 minutes at
672 37°C to remove 5' triphosphate groups. Library preparation and sequencing was
673 performed at the UNC School of Medicine High-Throughput Sequencing Facility
674 (HTSF). RNA-seq libraries were prepared using the NEXTflex Small RNA Library Prep
675 Kit for Illumina (Bio Scientific). Libraries were sequenced on an Illumina HiSeq 2500 to
676 produce approximately twenty million 50 bp single-end reads per library.
677
678 Analysis of high throughput sequencing data: Adapter trimming was performed as
679 required using the bbduk.sh script from the bbmap suite3 and custom scripts
680 (Bushnell, 2016). Reads were then filtered for 22G species or all species between 18
681 and 30 nucleotides in length using a custom python script. Reads were then converted
682 to fasta format and mapped to the *C. elegans* genome (WS251) using bowtie
683 (Langmead et al., 2009) with the following options: -M 1 -v 0 -best -strata. Uniquely
684 mapping sRNAs were detected by replacing the -M 1 parameter with -m 1. To detect

telomere-mapping sRNAs, reads were mapped to seven repeats of perfect telomere sequence (TTAGGC), allowing for zero mismatches. Unmapped reads were re-mapped to the telomere sequence, this time allowing for one mismatch. This step was repeated to detect reads that map to telomeres with two or three mismatches. Genes with differential sRNA abundance in *trt-1* were identified using DESeq2 (Love et al., 2014). To detect changes in the abundance of subtelomeric sRNAs in *trt-1* and *trt-1; dcr-1*, 22G reads mapping to the 2kb of sequence adjacent to the telomere were counted for each chromosome arm. Counts were normalized by dividing by the total number of mapped reads for each library. A pseudocount of 1 was added to each normalized value to avoid division by zero errors. Replicates were averaged and the log2-fold change between mutant and wildtype was calculated for each subtelomere. Analysis of sequencing data was performed using the R statistical computing environment(Team, 2017). Genome regions were visualized using the Gviz R package (Hahne and Ivanek, 2016). Immunoprecipitation datasets were used in Figure 3G, H but were excluded from the analysis shown in Figure 3D-F. To detect sRNAs targeting transposons, 22G reads were mapped to the *C. elegans* transposon consensus sequences downloaded from Repbase with bowtie, allowing for up to two mismatches. ChIP-seq reads were mapped to the genome as fastq files as described above without the size-filtering step. Read coverage was calculated at each base using bedtools (Quinlan and Hall, 2010). Coverage values were normalized by dividing by the number of total mapped reads for each library and enrichment was calculated by dividing the normalized coverage for IP libraries by the normalized coverage of their respective input libraries.

Accession numbers: RNA-seq data reported in this study are available under the accession number GEO: GSE111800.

**Acknowledgements**

We thank R. Dowen for technical advice with qRT-PCR, K. Billmyre for advice on immunofluorescence, and members of the S.A. laboratory for critical review of the manuscript. Some strains were provided by the *Caenorhabditis* Genetics Center, which is funded by National Institutes of Health Office of Research Infrastructure Programs

716 (P40 OD010440). S.F., C.L. and S.A. were supported by National Institute of Health
717 grant R01 GM135470.
718
719 **Competing Interests**
720 The authors declare no competing interests.

721 **References**
722

723 AHMED, S. & HODGKIN, J. 2000. MRT-2 checkpoint protein is required for germline
724 immortality and telomere replication in *C. elegans*. *Nature,* 403**,** 159-64.
725 AKAY, A., DI DOMENICO, T., SUEN, K. M., NABIH, A., PARADA, G. E., LARANCE, M.,
726 MEDHI, R., BERKYUREK, A. C., ZHANG, X., WEDELES, C. J., RUDOLPH, K. L.
727 M., ENGELHARDT, J., HEMBERG, M., MA, P., LAMOND, A. I.,
728 CLAYCOMB, J. M. & MISKA, E. A. 2017. The Helicase Aquarius/EMB-4 Is
729 Required to Overcome Intronic Barriers to Allow Nuclear RNAi Pathways to
730 Heritably Silence Transcription. *Dev Cell,* 42**,** 241-255 e6.
731 ARNOULT, N., VAN BENEDEN, A. & DECOTTIGNIES, A. 2012. Telomere length
732 regulates TERRA levels through increased trimethylation of telomeric H3K9 and
733 HP1alpha. *Nat Struct Mol Biol,* 19**,** 948-56.
734 ASHE, A., SAPETSCHNIG, A., WEICK, E. M., MITCHELL, J., BAGIJN, M. P.,
735 CORDING, A. C., DOEBLEY, A. L., GOLDSTEIN, L. D., LEHRBACH, N. J., LE
736 PEN, J., PINTACUDA, G., SAKAGUCHI, A., SARKIES, P., AHMED, S. & MISKA,
737 E. A. 2012. piRNAs Can Trigger a Multigenerational Epigenetic Memory in the
738 Germline of C. elegans. *Cell,* 150**,** 88-99.
739 AVGOUSTI, D. C., PALANI, S., SHERMAN, Y. & GRISHOK, A. 2012. CSR-1 RNAi
740 pathway positively regulates histone expression in C. elegans. *EMBO J,* 31**,** 3821-
741 32.
742 AZZALIN, C. M. & LINGNER, J. 2015. Telomere functions grounding on TERRA firma.
743 *Trends Cell Biol,* 25**,** 29-36.
744 AZZALIN, C. M., REICHENBACH, P., KHORIAULI, L., GIULOTTO, E. & LINGNER, J.
745 2007. Telomeric repeat containing RNA and RNA surveillance factors at
746 mammalian chromosome ends. *Science,* 318**,** 798-801.
747 BAGIJN, M. P., GOLDSTEIN, L. D., SAPETSCHNIG, A., WEICK, E. M., BOUASKER, S.,
748 LEHRBACH, N. J., SIMARD, M. J. & MISKA, E. A. 2012. Function, targets, and
749 evolution of Caenorhabditis elegans piRNAs. *Science,* 337**,** 574-8.
750 BATISTA, P. J., RUBY, J. G., CLAYCOMB, J. M., CHIANG, R., FAHLGREN, N.,
751 KASSCHAU, K. D., CHAVES, D. A., GU, W., VASALE, J. J., DUAN, S., CONTE,
752 D., JR., LUO, S., SCHROTH, G. P., CARRINGTON, J. C., BARTEL, D. P. &
753 MELLO, C. C. 2008. PRG-1 and 21U-RNAs interact to form the piRNA complex
754 required for fertility in C. elegans. *Mol Cell,* 31**,** 67-78.
755 BENETTI, R., GARCIA-CAO, M. & BLASCO, M. A. 2007. Telomere length regulates the
756 epigenetic status of mammalian telomeres and subtelomeres. *Nat Genet,* 39**,** 243-
757 50.
758 BENETTI, R., SCHOEFTNER, S., MUNOZ, P. & BLASCO, M. A. 2008. Role of TRF2 in
759 the assembly of telomeric chromatin. *Cell Cycle,* 7**,** 3461-8.
760 BERNSTEIN, E., CAUDY, A. A., HAMMOND, S. M. & HANNON, G. J. 2001. Role for a
761 bidentate ribonuclease in the initiation step of RNA interference. *Nature,* 409**,** 363-
762 6.
763 BILLI, A. C., FISCHER, S. E. & KIM, J. K. 2014. Endogenous RNAi pathways in C.
764 elegans. *WormBook***,** 1-49.

765 BOERCKEL, J., WALKER, D. & AHMED, S. 2007. The Caenorhabditis elegans Rad17
766 homolog HPR-17 is required for telomere replication. *Genetics,* 176**,** 703-9.
767 BUCKLEY, B. A., BURKHART, K. B., GU, S. G., SPRACKLIN, G., KERSHNER, A.,
768 FRITZ, H., KIMBLE, J., FIRE, A. & KENNEDY, S. 2012. A nuclear Argonaute
769 promotes multigenerational epigenetic inheritance and germline immortality.
770 *Nature,* 489**,** 447-51.
771 BUSHNELL, B. 2016. BBMap short-read aligner, and other bioinformatics tools.
772 http://sourceforge.net/projects/bbmap/.
773 CANZIO, D., LARSON, A. & NARLIKAR, G. J. 2014. Mechanisms of functional
774 promiscuity by HP1 proteins. *Trends Cell Biol,* 24**,** 377-86.
775 CAO, F., LI, X., HIEW, S., BRADY, H., LIU, Y. & DOU, Y. 2009. Dicer independent small
776 RNAs associate with telomeric heterochromatin. *RNA,* 15**,** 1274-81. CHAVEZ, J.,
777 MURILLO-MALDONADO, J. M., BAHENA, V., CRUZ, A. K., CASTANEDA-SORTIBRAN,
778 A., RODRIGUEZ-ARNAIZ, R., ZURITA, M. & VALADEZ-GRAHAM, V. 2017. dAdd1 and
779 dXNP prevent genome instability by maintaining HP1a localization at Drosophila
780 telomeres. *Chromosoma,* 126**,** 697712.
781 CHENG, C., SHTESSEL, L., BRADY, M. M. & AHMED, S. 2012. Caenorhabditis elegans
782 POT-2 telomere protein represses a mode of alternative lengthening of telomeres
783 with normal telomere lengths. *Proc Natl Acad Sci U S A,* 109**,** 7805-10.
784 CHU, H. P., CIFUENTES-ROJAS, C., KESNER, B., AEBY, E., LEE, H. G., WEI, C., OH,
785 H. J., BOUKHALI, M., HAAS, W. & LEE, J. T. 2017. TERRA RNA Antagonizes
786 ATRX and Protects Telomeres. *Cell,* 170**,** 86-101 e16.
787 CLAYCOMB, J.M., BATISTA, P.J., PANG, K.M., GU, W., VASALE, J.J., VAN
788 WOLFSWINKEL, J.C., CHAVES, D.A., SHIRAYAMA, M., MITANI, S., KETTING, R.F.,
789 CONTE D., MELLO C.C. (2009). The Argonaute CSR-1 and its 22G-RNA cofactors are
790 required for holocentric chromosome segregation. *Cell* 139, 123-134.
791 COUVILLION, M. T., LEE, S. R., HOGSTAD, B., MALONE, C. D., TONKIN, L. A.,
792 SACHIDANANDAM, R., HANNON, G. J. & COLLINS, K. 2009. Sequence,
793 biogenesis, and function of diverse small RNA classes bound to the Piwi family
794 proteins of Tetrahymena thermophila. *Genes Dev,* 23**,** 2016-32.
795 CUSANELLI, E., ROMERO, C. A. & CHARTRAND, P. 2013. Telomeric noncoding RNA
796 TERRA is induced by telomere shortening to nucleate telomerase molecules at
797 short telomeres. *Mol Cell,* 51**,** 780-91.
798 DAS, P. P., BAGIJN, M. P., GOLDSTEIN, L. D., WOOLFORD, J. R., LEHRBACH, N. J.,
799 SAPETSCHNIG, A., BUHECHA, H. R., GILCHRIST, M. J., HOWE, K. L.,
800 STARK, R., MATTHEWS, N., BEREZIKOV, E., KETTING, R. F., TAVARE, S. &
801 MISKA, E. A. 2008. Piwi and piRNAs act upstream of an endogenous siRNA
802 pathway to suppress Tc3 transposon mobility in the Caenorhabditis elegans
803 germline. *Mol Cell,* 31**,** 79-90.
804 DONATE, L. E. & BLASCO, M. A. 2011. Telomeres in cancer and ageing. *Philos Trans R*
805 *Soc Lond B Biol Sci,* 366**,** 76-84.
806 FANTI, L., GIOVINAZZO, G., BERLOCO, M. & PIMPINELLI, S. 1998. The
807 heterochromatin protein 1 prevents telomere fusions in Drosophila. *Mol Cell,* 2**,**
808 527-38.

809 FLYNN, R. L., COX, K. E., JEITANY, M., WAKIMOTO, H., BRYLL, A. R., GANEM, N.
810 J., BERSANI, F., PINEDA, J. R., SUVA, M. L., BENES, C. H., HABER, D. A.,
811 BOUSSIN, F. D. & ZOU, L. 2015. Alternative lengthening of telomeres renders
812 cancer cells hypersensitive to ATR inhibitors. *Science,* 347**,** 273-7.
813 FRENK, S., LISTER-SHIMAUCHI, E. H. & AHMED, S. 2019. Telomeric small RNAs in
814 the genus Caenorhabditis. *RNA*.
815 FULCHER, N., DERBOVEN, E., VALUCHOVA, S. & RIHA, K. 2014. If the cap fits, wear
816 it: an overview of telomeric structures over evolution. *Cell Mol Life Sci,* 71**,** 84765.
817 GENT, J. I., LAMM, A. T., PAVELEC, D. M., MANIAR, J. M., PARAMESWARAN, P., TAO,
818 L., KENNEDY, S. & FIRE, A. Z. 2010. Distinct phases of siRNA synthesis in an
819 endogenous RNAi pathway in C. elegans soma. *Mol Cell,* 37**,** 679-89.
820 GOU, L. T., DAI, P., YANG, J. H., XUE, Y., HU, Y. P., ZHOU, Y., KANG, J. Y., WANG, X.,
821 LI, H., HUA, M. M., ZHAO, S., HU, S. D., WU, L. G., SHI, H. J., LI, Y., FU, X. D.,
822 QU, L. H., WANG, E. D. & LIU, M. F. 2014. Pachytene piRNAs instruct massive
823 mRNA elimination during late spermiogenesis. *Cell Res,* 24**,** 680-700.
824 GRAF, M., BONETTI, D., LOCKHART, A., SERHAL, K., KELLNER, V., MAICHER, A.,
825 JOLIVET, P., TEIXEIRA, M. T. & LUKE, B. 2017. Telomere Length Determines
826 TERRA and R-Loop Regulation through the Cell Cycle. *Cell,* 170**,** 72-85 e14.
827 GREER, E. L., MAURES, T. J., HAUSWIRTH, A. G., GREEN, E. M., LEEMAN, D. S.,
828 MARO, G. S., HAN, S., BANKO, M. R., GOZANI, O. & BRUNET, A. 2010.
829 Members of the H3K4 trimethylation complex regulate lifespan in a
830 germlinedependent manner in C. elegans. *Nature,* 466**,** 383-7.
831 GU, W., SHIRAYAMA, M., CONTE, D., JR., VASALE, J., BATISTA, P. J., CLAYCOMB,
832 J. M., MORESCO, J. J., YOUNGMAN, E. M., KEYS, J., STOLTZ, M. J., CHEN,
833 C. C., CHAVES, D. A., DUAN, S., KASSCHAU, K. D., FAHLGREN, N., YATES, J.
834 R., 3RD, MITANI, S., CARRINGTON, J. C. & MELLO, C. C. 2009. Distinct
835 argonaute-mediated 22G-RNA pathways direct genome surveillance in the C.
836 elegans germline. *Mol Cell,* 36**,** 231-44.
837 HAHNE, F. & IVANEK, R. 2016. Visualizing Genomic Data Using Gviz and Bioconductor.
838 *Methods Mol Biol,* 1418**,** 335-51.
839 HAN, T., MANOHARAN, A. P., HARKINS, T. T., BOUFFARD, P., FITZPATRICK, C., CHU,
840 D. S., THIERRY-MIEG, D., THIERRY-MIEG, J. & KIM, J. K. 2009. 26G endo-
841 siRNAs regulate spermatogenic and zygotic gene expression in Caenorhabditis
842 elegans. *Proc Natl Acad Sci U S A,* 106**,** 18674-9.
843 HEARD, E. & TURNER, J. 2011. Function of the sex chromosomes in mammalian
844 fertility. *Cold Spring Harb Perspect Biol,* 3**,** a002675.
845 HOLOCH, D. & MOAZED, D. 2015. RNA-mediated epigenetic regulation of gene
846 expression. *Nat Rev Genet,* 16**,** 71-84.
847 HOLOHAN, B., WRIGHT, W. E. & SHAY, J. W. 2014. Cell biology of disease:
848 Telomeropathies: an emerging spectrum disorder. *J Cell Biol,* 205**,** 289-99.
849 JANSSEN, A., COLMENARES, S. U. & KARPEN, G. H. 2018. Heterochromatin:
850 Guardian of the Genome. *Annu Rev Cell Dev Biol,* 34**,** 265-288.
851 KASPER, D. M., GARDNER, K. E. & REINKE, V. 2014. Homeland security in the C.

elegans germ line: insights into the biogenesis and function of piRNAs. *Epigenetics,* 9**,** 62-74.

KETTING, R. F., FISCHER, S. E., BERNSTEIN, E., SIJEN, T., HANNON, G. J. & PLASTERK, R. H. 2001. Dicer functions in RNA interference and in synthesis of small RNA involved in developmental timing in C. elegans. *Genes Dev,* 15**,** 26549.

KETTING, R. F., HAVERKAMP, T. H., VAN LUENEN, H. G. & PLASTERK, R. H. 1999. Mut-7 of C. elegans, required for transposon silencing and RNA interference, is a homolog of Werner syndrome helicase and RNaseD. *Cell,* 99**,** 133-41.

KNIGHT, S. W. & BASS, B. L. 2001. A role for the RNase III enzyme DCR-1 in RNA interference and germ line development in Caenorhabditis elegans. *Science,* 293**,** 2269-71.

LANGMEAD, B., TRAPNELL, C., POP, M. & SALZBERG, S. L. 2009. Ultrafast and memory-efficient alignment of short DNA sequences to the human genome. *Genome Biol,* 10**,** R25.

LI, F., HUARTE, M., ZARATIEGUI, M., VAUGHN, M. W., SHI, Y., MARTIENSSEN, R. & CANDE, W. Z. 2008. Lid2 is required for coordinating H3K4 and H3K9 methylation of heterochromatin and euchromatin. *Cell,* 135**,** 272-83.

LI, J. S., MIRALLES FUSTE, J., SIMAVORIAN, T., BARTOCCI, C., TSAI, J., KARLSEDER, J. & LAZZERINI DENCHI, E. 2017. TZAP: A telomere-associated protein involved in telomere length control. *Science,* 355**,** 638-641.

LOVE, M. I., HUBER, W. & ANDERS, S. 2014. Moderated estimation of fold change and dispersion for RNA-seq data with DESeq2. *Genome Biol,* 15**,** 550.

LOVEJOY, C. A., LI, W., REISENWEBER, S., THONGTHIP, S., BRUNO, J., DE LANGE, T., DE, S., PETRINI, J. H., SUNG, P. A., JASIN, M., ROSENBLUH, J., ZWANG, Y., WEIR, B. A., HATTON, C., IVANOVA, E., MACCONAILL, L., HANNA, M., HAHN, W. C., LUE, N. F., REDDEL, R. R., JIAO, Y., KINZLER, K., VOGELSTEIN, B., PAPADOPOULOS, N., MEEKER, A. K. & CONSORTIUM, A. L. T. S. C. 2012. Loss of ATRX, genome instability, and an altered DNA damage response are hallmarks of the alternative lengthening of telomeres pathway. *PLoS Genet,* 8**,** e1002772.

MACIEJOWSKI, J. & DE LANGE, T. 2017. Telomeres in cancer: tumour suppression and genome instability. *Nat Rev Mol Cell Biol,* 18**,** 175-186.

MAICHER, A., KASTNER, L., DEES, M. & LUKE, B. 2012. Deregulated telomere transcription causes replication-dependent telomere shortening and promotes cellular senescence. *Nucleic Acids Res,* 40**,** 6649-59.

MARION, R. M., MONTERO, J. J., LOPEZ DE SILANES, I., GRANA-CASTRO, O., MARTINEZ, P., SCHOEFTNER, S., PALACIOS-FABREGA, J. A. & BLASCO, M. A. 2019. TERRA regulate the transcriptional landscape of pluripotent cells through TRF1-dependent recruitment of PRC2. *Elife,* 8.

MCMURCHY, A. N., STEMPOR, P., GAARENSTROOM, T., WYSOLMERSKI, B., DONG, Y., AUSSIANIKAVA, D., APPERT, A., HUANG, N., KOLASINSKAZWIERZ, P., SAPETSCHNIG, A., MISKA, E. A. & AHRINGER, J. 2017. A team of heterochromatin factors collaborates with small RNA pathways to combat repetitive elements and germline stress. *Elife,* 6.

MEIER, B., BARBER, L. J., LIU, Y., SHTESSEL, L., BOULTON, S. J., GARTNER, A. & AHMED, S. 2009. The MRT-1 nuclease is required for DNA crosslink repair and telomerase activity in vivo in Caenorhabditis elegans. *Embo J,* 28**,** 3549-63.

MEIER, B., CLEJAN, I., LIU, Y., LOWDEN, M., GARTNER, A., HODGKIN, J. & AHMED, S. 2006. trt-1 is the Caenorhabditis elegans catalytic subunit of telomerase. *PLoS Genet,* 2**,** e18.

MONTERO, J. J., LOPEZ-SILANES, I., MEGIAS, D., M, F. F., CASTELLS-GARCIA, A. & BLASCO, M. A. 2018. TERRA recruitment of polycomb to telomeres is essential for histone trymethylation marks at telomeric heterochromatin. *Nat Commun,* 9**,** 1548.

MORAVEC, M., WISCHNEWSKI, H., BAH, A., HU, Y., LIU, N., LAFRANCHI, L., KING, M. C. & AZZALIN, C. M. 2016. TERRA promotes telomerase-mediated telomere elongation in Schizosaccharomyces pombe. *EMBO Rep,* 17**,** 999-1012.

ORTIZ, M. A., NOBLE, D., SOROKIN, E. P. & KIMBLE, J. 2014. A new dataset of spermatogenic vs. oogenic transcriptomes in the nematode Caenorhabditis elegans. *G3 (Bethesda),* 4**,** 1765-72.

PAK, J. & FIRE, A. 2007. Distinct populations of primary and secondary effectors during RNAi in C. elegans. *Science,* 315**,** 241-4.

PANE, A., WEHR, K. & SCHUPBACH, T. 2007. zucchini and squash encode two putative nucleases required for rasiRNA production in the Drosophila germline. *Dev Cell,* 12**,** 851-62.

PARDUE, M. L. & DEBARYSHE, P. G. 2003. Retrotransposons provide an evolutionarily robust non-telomerase mechanism to maintain telomeres. *Annu Rev Genet,* 37**,** 485-511.

PERRINI, B., PIACENTINI, L., FANTI, L., ALTIERI, F., CHICHIARELLI, S., BERLOCO, M., TURANO, C., FERRARO, A. & PIMPINELLI, S. 2004. HP1 controls telomere capping, telomere elongation, and telomere silencing by two different mechanisms in Drosophila. *Mol Cell,* 15**,** 467-76.

PFEIFFER, V. & LINGNER, J. 2012. TERRA promotes telomere shortening through exonuclease 1-mediated resection of chromosome ends. *PLoS Genet,* 8**,** e1002747.

PHILLIPS, C. M., MCDONALD, K. L. & DERNBURG, A. F. 2009. Cytological analysis of meiosis in Caenorhabditis elegans. *Methods Mol Biol,* 558**,** 171-95.

PICKETT, H. A. & REDDEL, R. R. 2015. Molecular mechanisms of activity and derepression of alternative lengthening of telomeres. *Nat Struct Mol Biol,* 22**,** 875-80.

POLO, S. E. & JACKSON, S. P. 2011. Dynamics of DNA damage response proteins at DNA breaks: a focus on protein modifications. *Genes Dev,* 25**,** 409-33.

PORRO, A., FEUERHAHN, S., DELAFONTAINE, J., RIETHMAN, H., ROUGEMONT, J. & LINGNER, J. 2014. Functional characterization of the TERRA transcriptome at damaged telomeres. *Nat Commun,* 5**,** 5379.

QUINLAN, A. R. & HALL, I. M. 2010. BEDTools: a flexible suite of utilities for comparing genomic features. *Bioinformatics,* 26**,** 841-2.

939 REINHART, B. J. & BARTEL, D. P. 2002. Small RNAs correspond to centromere
940 heterochromatic repeats. *Science,* 297**,** 1831.
941 ROAKE, C. M. & ARTANDI, S. E. 2017. Approaching TERRA Firma: Genomic Functions
942 of Telomeric Noncoding RNA. *Cell,* 170**,** 8-9.
943 ROSSIELLO, F., AGUADO, J., SEPE, S., IANNELLI, F., NGUYEN, Q., PITCHIAYA, S.,
944 CARNINCI, P. & D'ADDA DI FAGAGNA, F. 2017. DNA damage response
945 inhibition at dysfunctional telomeres by modulation of telomeric DNA damage
946 response RNAs. *Nat Commun,* 8**,** 13980.
947 SAGIE, S., TOUBIANA, S., HARTONO, S. R., KATZIR, H., TZUR-GILAT, A.,
948 HAVAZELET, S., FRANCASTEL, C., VELASCO, G., CHEDIN, F. & SELIG, S.
949 2017. Telomeres in ICF syndrome cells are vulnerable to DNA damage due to
950 elevated DNA:RNA hybrids. *Nat Commun,* 8**,** 14015.
951 SAKAGUCHI, A., SARKIES, P., SIMON, M., DOEBLEY, A. L., GOLDSTEIN, L. D.,
952 HEDGES, A., IKEGAMI, K., ALVARES, S. M., YANG, L., LAROCQUE, J. R.,
953 HALL, J., MISKA, E. A. & AHMED, S. 2014. Caenorhabditis elegans RSD-2 and
954 RSD-6 promote germ cell immortality by maintaining small interfering RNA
955 populations. *Proc Natl Acad Sci U S A,* 111**,** E4323-31.
956 SARIN, K. Y., CHEUNG, P., GILISON, D., LEE, E., TENNEN, R. I., WANG, E., ARTANDI,
957 M. K., ORO, A. E. & ARTANDI, S. E. 2005. Conditional telomerase induction
958 causes proliferation of hair follicle stem cells. *Nature,* 436**,** 1048-52.
959 SAVITSKY, M., KWON, D., GEORGIEV, P., KALMYKOVA, A. & GVOZDEV, V. 2006.
960 Telomere elongation is under the control of the RNAi-based mechanism in the
961 Drosophila germline. *Genes Dev,* 20**,** 345-54.
962 SCHAETZLEIN, S., KODANDARAMIREDDY, N. R., JU, Z., LECHEL, A.,
963 STEPCZYNSKA, A., LILLI, D. R., CLARK, A. B., RUDOLPH, C., KUHNEL, F.,
964 WEI, K., SCHLEGELBERGER, B., SCHIRMACHER, P., KUNKEL, T. A.,
965 GREENBERG, R. A., EDELMANN, W. & RUDOLPH, K. L. 2007. Exonuclease-1
966 deletion impairs DNA damage signaling and prolongs lifespan of
967 telomeredysfunctional mice. *Cell,* 130**,** 863-77.
968 SHAY, J. W. 2016. Role of Telomeres and Telomerase in Aging and Cancer. *Cancer*
969 *Discov,* 6**,** 584-93.
970 SHIMAMOTO, A., YOKOTE, K. & TAHARA, H. 2015. Werner Syndrome-specific induced
971 pluripotent stem cells: recovery of telomere function by reprogramming. *Front*
972 *Genet,* 6**,** 10.
973 SHIRAYAMA, M., STANNEY, W., 3RD, GU, W., SETH, M. & MELLO, C. C. 2014. The
974 Vasa Homolog RDE-12 engages target mRNA and multiple argonaute proteins to
975 promote RNAi in C. elegans. *Curr Biol,* 24**,** 845-51.
976 STEINER, F. A., OKIHARA, K. L., HOOGSTRATE, S. W., SIJEN, T. & KETTING, R. F.
977 2009. RDE-1 slicer activity is required only for passenger-strand cleavage during
978 RNAi in Caenorhabditis elegans. *Nat Struct Mol Biol,* 16**,** 207-11.
979 TABARA, H., YIGIT, E., SIOMI, H. & MELLO, C. C. 2002. The dsRNA binding protein
980 RDE-4 interacts with RDE-1, DCR-1, and a DExH-box helicase to direct RNAi in
981 C. elegans. *Cell,* 109**,** 861-71.

TAYLOR, D. H., CHU, E. T., SPEKTOR, R. & SOLOWAY, P. D. 2015. Long non-coding RNA regulation of reproduction and development. *Mol Reprod Dev,* 82**,** 932-56.

TEAM, R. C. 2017. R: A language and environment for statistical computing. R Foundation for Statistical Computing, Vienna, Austria. https://www.R-project.org/.

TIJSTERMAN, M., KETTING, R. F., OKIHARA, K. L., SIJEN, T. & PLASTERK, R. H. 2002. RNA helicase MUT-14-dependent gene silencing triggered in C. elegans by short antisense RNAs. *Science,* 295**,** 694-7.

TOUBIANA, S. & SELIG, S. 2018. DNA:RNA hybrids at telomeres - when it is better to be out of the (R) loop. *FEBS J,* 285**,** 2552-2566.

UDUGAMA, M., FT, M. C., CHAN, F. L., TANG, M. C., PICKETT, H. A., JD, R. M., MAYNE, L., COLLAS, P., MANN, J. R. & WONG, L. H. 2015. Histone variant H3.3 provides the heterochromatic H3 lysine 9 tri-methylation mark at telomeres. *Nucleic Acids Res,* 43**,** 10227-37.

VRBSKY, J., AKIMCHEVA, S., WATSON, J. M., TURNER, T. L., DAXINGER, L., VYSKOT, B., AUFSATZ, W. & RIHA, K. 2010. siRNA-mediated methylation of Arabidopsis telomeres. *PLoS Genet,* 6**,** e1000986.

WANAT, J. J., LOGSDON, G. A., DRISKILL, J. H., DENG, Z., LIEBERMAN, P. M. & JOHNSON, F. B. 2018. TERRA and the histone methyltransferase Dot1 cooperate to regulate senescence in budding yeast. *PLoS One,* 13**,** e0195698.

WEDELES, C. J., WU, M. Z. & CLAYCOMB, J. M. 2013. Protection of germline gene expression by the C. elegans Argonaute CSR-1. *Dev Cell,* 27**,** 664-71.

WELKER, N. C., PAVELEC, D. M., NIX, D. A., DUCHAINE, T. F., KENNEDY, S. & BASS, B. L. 2010. Dicer's helicase domain is required for accumulation of some, but not all, C. elegans endogenous siRNAs. *RNA,* 16**,** 893-903.

WICKY, C., VILLENEUVE, A. M., LAUPER, N., CODOUREY, L., TOBLER, H. & MULLER, F. 1996. Telomeric repeats (TTAGGC)n are sufficient for chromosome capping function in Caenorhabditis elegans. *Proc Natl Acad Sci U S A,* 93**,** 89838.

WONG, L. H., MCGHIE, J. D., SIM, M., ANDERSON, M. A., AHN, S., HANNAN, R. D., GEORGE, A. J., MORGAN, K. A., MANN, J. R. & CHOO, K. H. 2010. ATRX interacts with H3.3 in maintaining telomere structural integrity in pluripotent embryonic stem cells. *Genome Res,* 20**,** 351-60.

ZELLER, P., PADEKEN, J., VAN SCHENDEL, R., KALCK, V., TIJSTERMAN, M. & GASSER, S. M. 2016. Histone H3K9 methylation is dispensable for Caenorhabditis elegans development but suppresses RNA:DNA hybridassociated repeat instability. *Nat Genet,* 48**,** 1385-1395.

ZHANG, W., LI, J., SUZUKI, K., QU, J., WANG, P., ZHOU, J., LIU, X., REN, R., XU, X., OCAMPO, A., YUAN, T., YANG, J., LI, Y., SHI, L., GUAN, D., PAN, H., DUAN, S., DING, Z., LI, M., YI, F., BAI, R., WANG, Y., CHEN, C., YANG, F., LI, X., WANG, Z., AIZAWA, E., GOEBL, A., SOLIGALLA, R. D., REDDY, P., ESTEBAN, C. R., TANG, F., LIU, G. H. & BELMONTE, J. C. 2015. Aging stem cells. A Werner syndrome stem cell model unveils heterochromatin alterations as a driver of human aging. *Science,* 348**,** 1160-3.

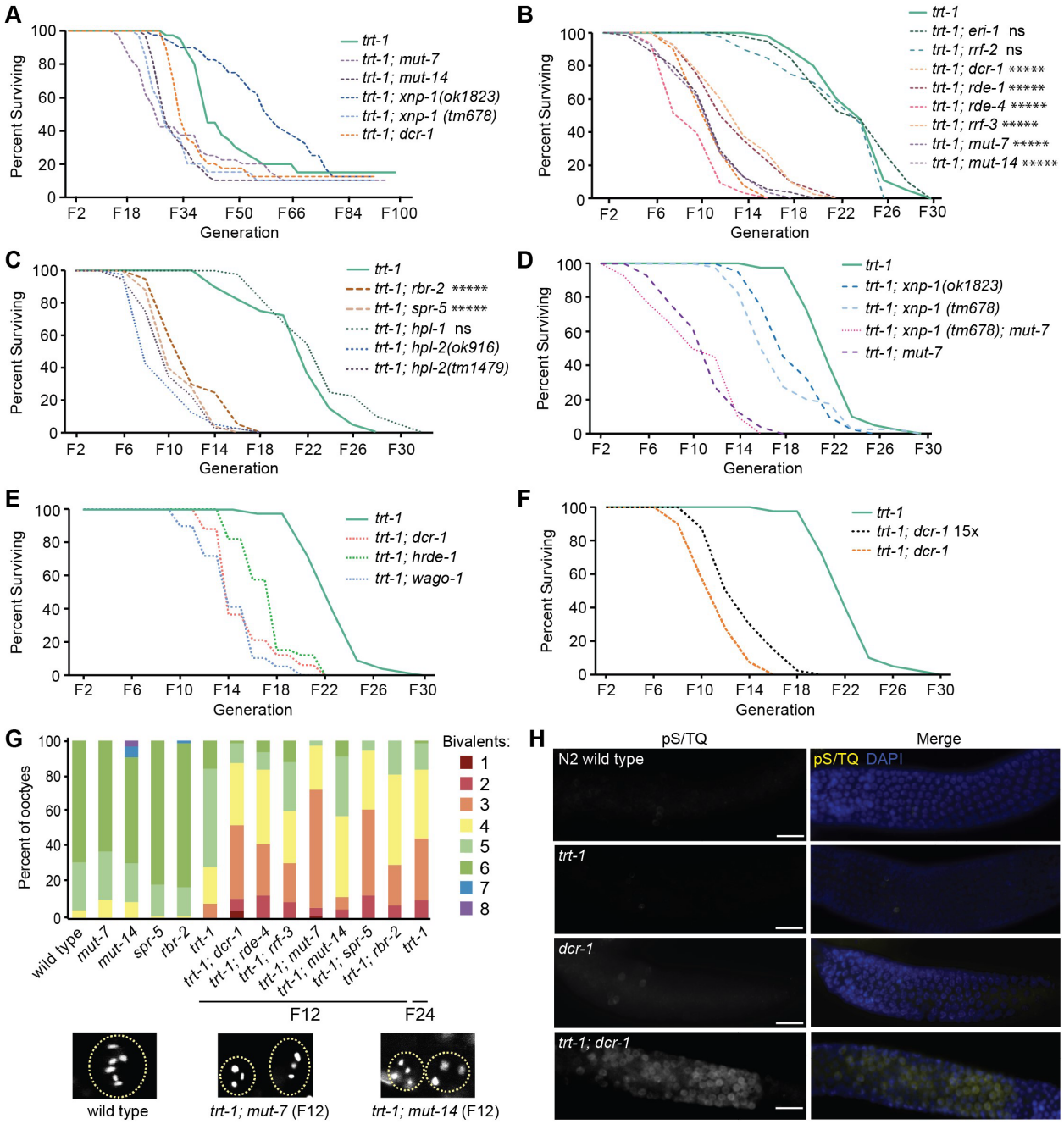


**Figure 1**: Endogenous small RNA and chromatin factors repress telomere stability in the absence of telomerase. (A) Survival curve of telomerase-deficient strains passaged at ~100 worms weekly for 40 independent lines. One allele of *xnp-1(ok1823)* extended survival but did not increase survival via ALT (Table S1). The same wild type control data is shown in panels B-F. (B) Survival curve of primary or secondary sRNA deficient telomerase mutants when 6 larval L1s are passaged weekly. (C) Survival curve of

1036 double mutants for *trt-1* and chromatin factors passaged by 6 L1s weekly. (D) Histone
1037 H3.3 remodeling protein XNP-1 represses senescence in *trt-1* mutants epistatically to
1038 the small RNA factor MUT-7. (E) Loss of HRDE-1 or WAGO-1 Argonaute proteins
1039 mimics the accelerated sterility observed in a *trt-1; dcr-1* mutant background. (F) A *trt-*
1040 *1; dcr-1* strain was crossed with *dcr-1* males fifteen times to yield a *trt-1; dcr-1* 15x strain
1041 that displayed the same accelerated sterility observed for the initial *trt-1; dcr-1* double
1042 mutants. (G) Small RNA and heterochromatin mutant *trt-1* lines have high levels of
1043 chromosome fusions, comparable to *trt-1* single mutants at F24. Fusions were assayed
1044 by diamidino-2-phenylindole (DAPI) staining of oocytes in diakinesis. Each bivalent in
1045 wildtype represents a single paired chromosome. Representative images of
1046 DAPIstained oocyte nuclei are shown in panels below the graph. (H) High levels of
1047 phospho(Ser/Thr) staining in the meiotic gonad of *trt-1; dcr-1* at F6 compared to N2 or
1048 *trt-1*. Scale bar, 25 m. (B)-(D), (F) ***$p < 0.001$; ****$p < 0.00001$; ns, not significant, (Log
1049 rank test, n=40 independent lines for each genotype). (E) *trt-1; wago-1* = 39 lines per
1050 genotype. *trt-1; hrde-1* and *trt-1; dcr-1* = 33 lines per genotype.
1051

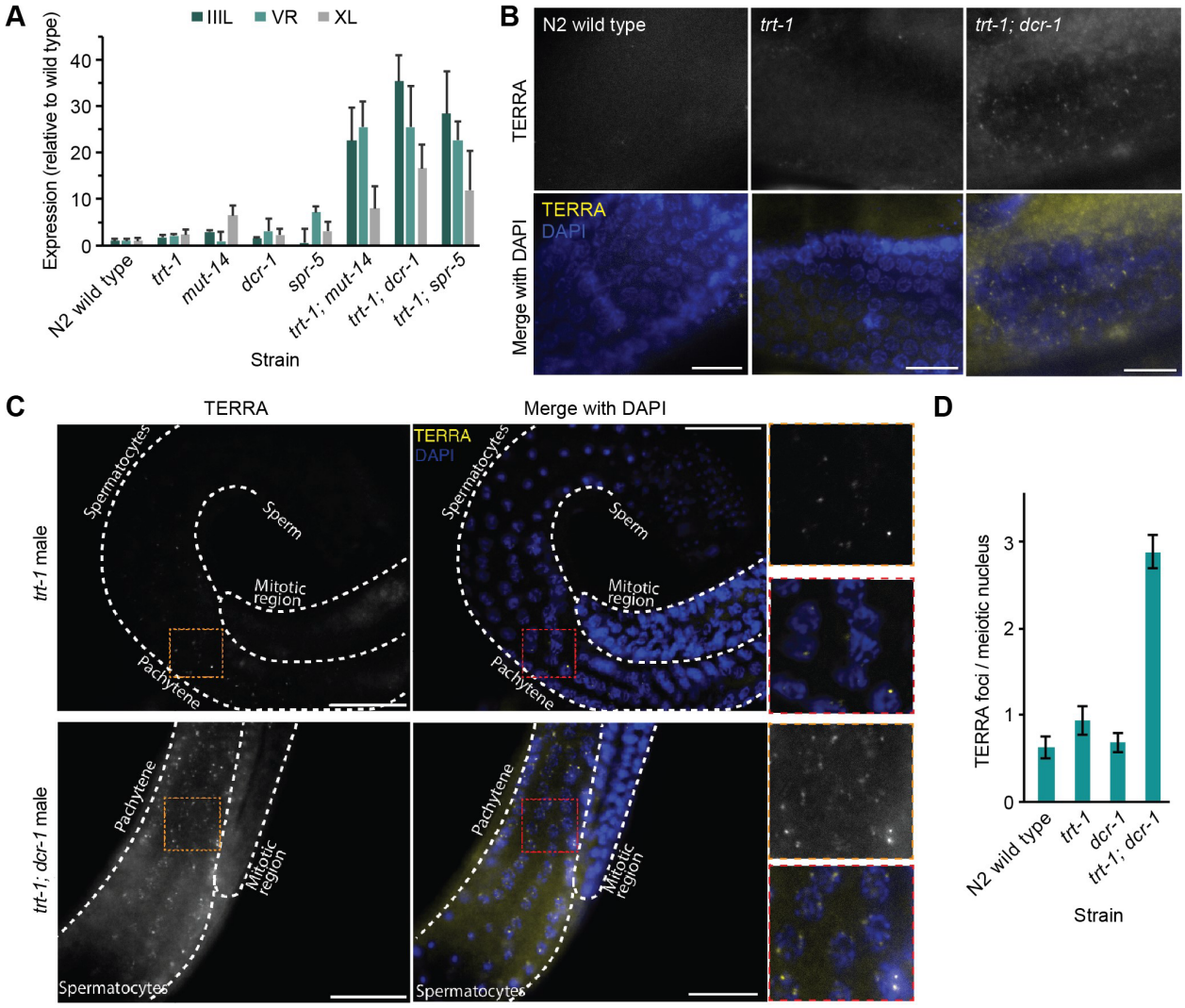


**Figure 2:** (A) Expression of TERRA from subtelomeres *IIIL*, *VR*, and *XL* is increased in sRNA and heterochromatin deficient telomerase mutants. cDNA was reverse transcribed with a telomere specific primer and qPCR was performed using subtelomere-specific primer pairs and normalized to *act-1*. Expression data are plotted relative to wildtype and represent the mean ± SEM of three biological replicates. (B) RNA FISH signals of TERRA in meiotic germlines of hermaphrodites of the indicated genotypes. TERRA foci are present in wildtype and *trt-1* in the pachytene region and increased in *trt-1; dcr-1.* Scale bar, 10um. (C) Representative RNA FISH images of TERRA in males show foci in the pachytene region of the germline which are increased in *trt-1; dcr-1* compared to *trt-1.* Scale bar, 20 um. (D) Quantification of germline TERRA foci (mean ± SEM, n=10 germlines).

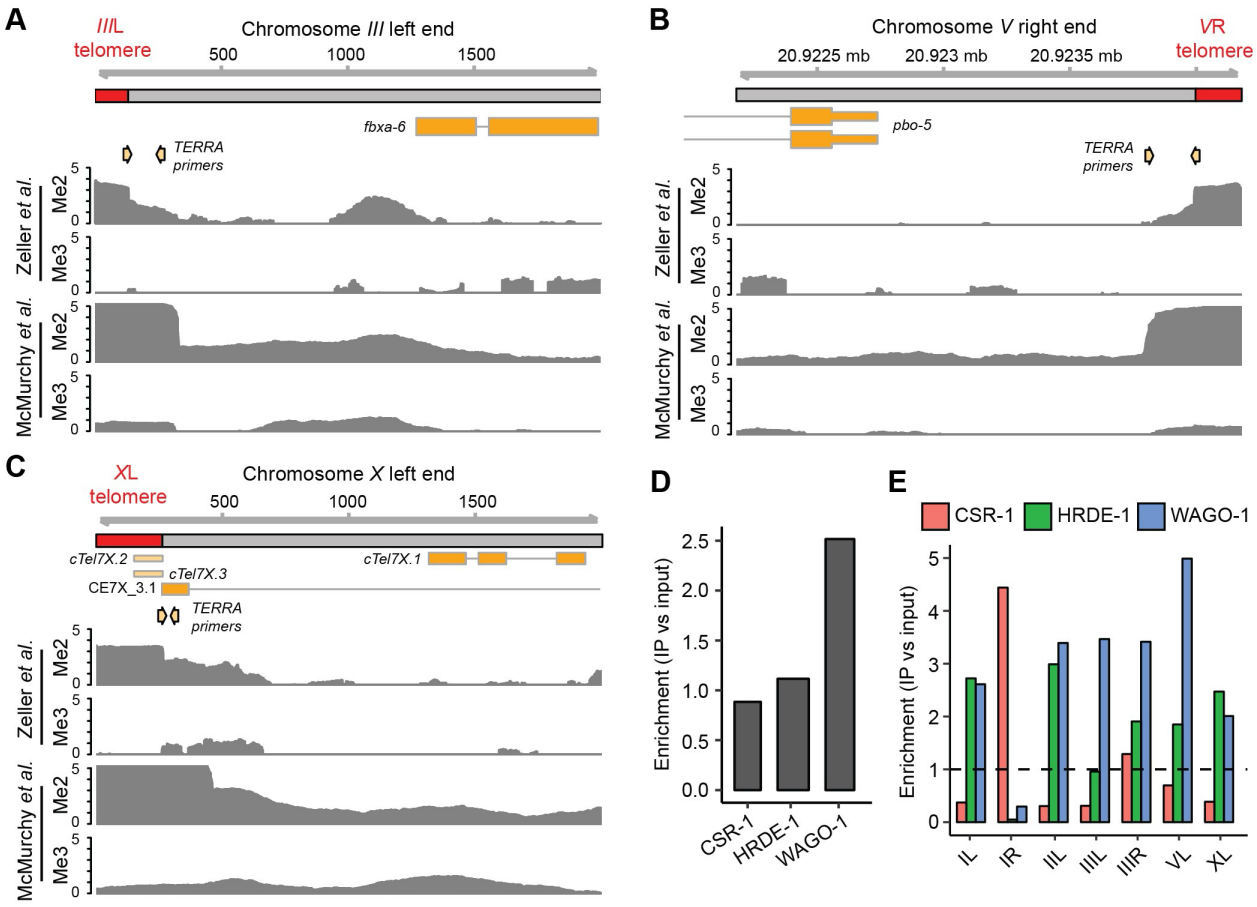


**Figure 3:** Analysis of telomeric chromatin and small RNAs in published datasets. (A)(C) ChIP-seq enrichment profiles at three chromosome ends constructed using published data (McMurchy et al., 2017, Zeller et al., 2016). Small orange arrows between gene models and data tracks show the position of primers used in TERRA qRT-PCR experiments. (D) Enrichment (IP/input) of reads mapping to perfect telomere sequence with up to three mismatches in published immunoprecipitation datasets for three different Argonaute proteins. (E) Enrichment for subtelomeric sRNAs for datasets used in (D).

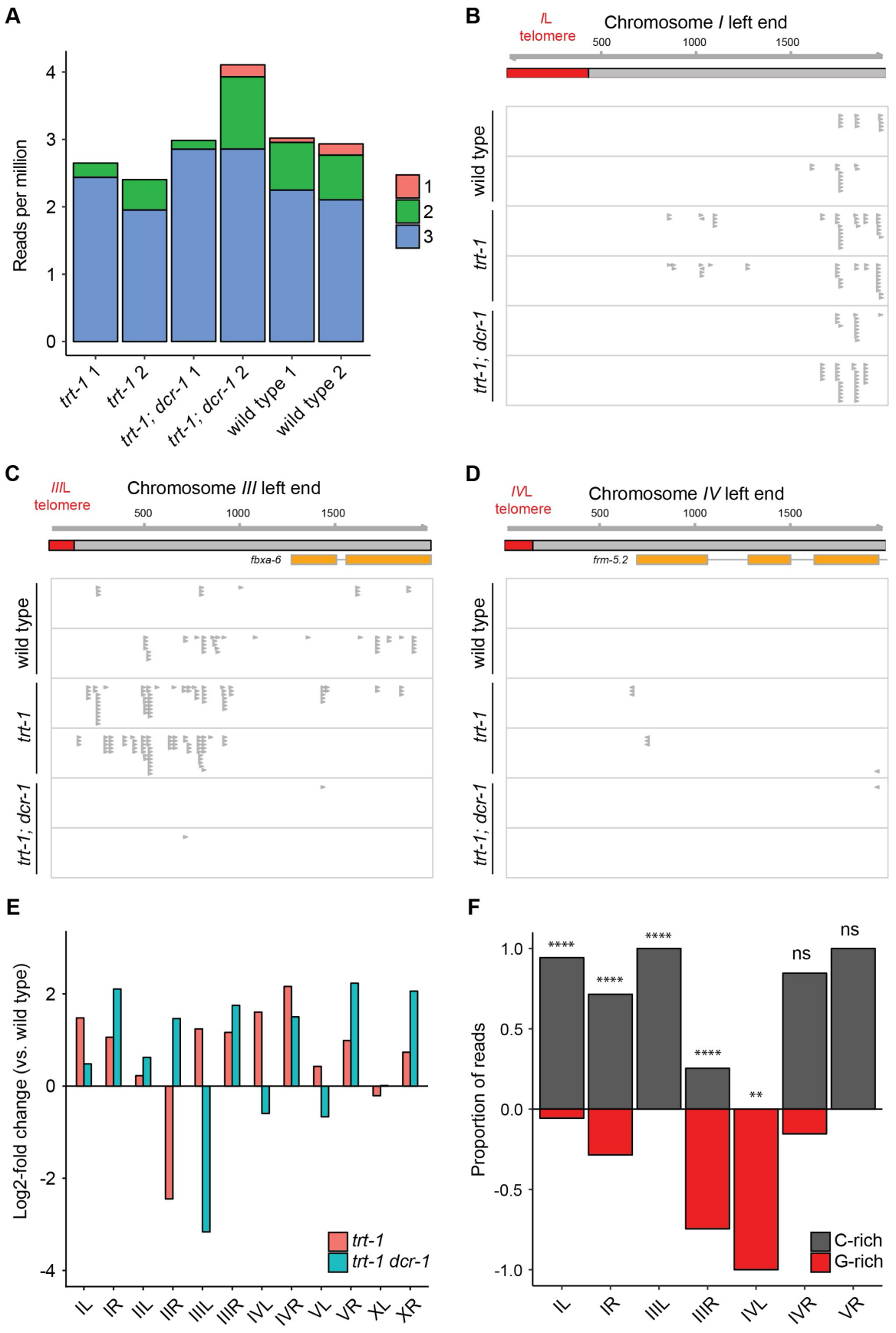
A
Reads per million
0
1
2
3
4
trt-1 1
trt-1 2
trt-1; dcr-1 1
trt-1; dcr-1 2
wild type 1
wild type 2
1
2
3
B
IL telomere
Chromosome I left end
500
1000
1500
wild type
trt-1
trt-1; dcr-1
C
IIIL telomere
Chromosome III left end
500
1000
1500
fbxa-6
wild type
trt-1
trt-1; dcr-1
D
IVL telomere
Chromosome IV left end
500
1000
1500
frm-5.2
wild type
trt-1
trt-1; dcr-1
E
Log2-fold change (vs. wild type)
-4
-2
0
2
trt-1
trt-1 dcr-1
IL
IR
IIL
IIR
IIIL
IIIR
IVL
IVR
VL
VR
XL
XR
F
Proportion of reads
-1.0
-0.5
0.0
0.5
1.0
****
****
****
****
**
ns
ns
C-rich
G-rich
IL
IR
IIIL
IIIR
IVL
IVR
VR

1081

1082
1083 **Figure 4:** Upregulation of subtelomeric sRNAs in telomerase mutants. (A) Number of
1084 telomere-mapping reads in wild-type, *trt-1,* and *trt-1;dcr-1* libraries. Numbers 1-3
1085 indicate number of mismatches. (B)-(D) 22G sRNAs at three subtelomeres. (E)
1086 Log2fold change in sRNA abundance at subtelomeres relative to wildtype in *trt-1* and
1087 *trt-1; dcr-1* animals. (F) Proportion of subtelomeric sRNAs mapping to the strand
1088 corresponding to the G-rich (TTAGGC) and C-rich (TAAGCC) telomere strand in *trt-1*
1089 animals. **** $p < 0.0001$; ** $p < 0.01$; ns, not significant (Binomial test with Bonferroni
1090 correction). The p values refer to the probability of observing the given proportion of G-rich
1091 or C-rich telomeric reads at each chromosome end under the null hypothesis that G- and C-
1092 rich reads are present in equal proportions.
1093

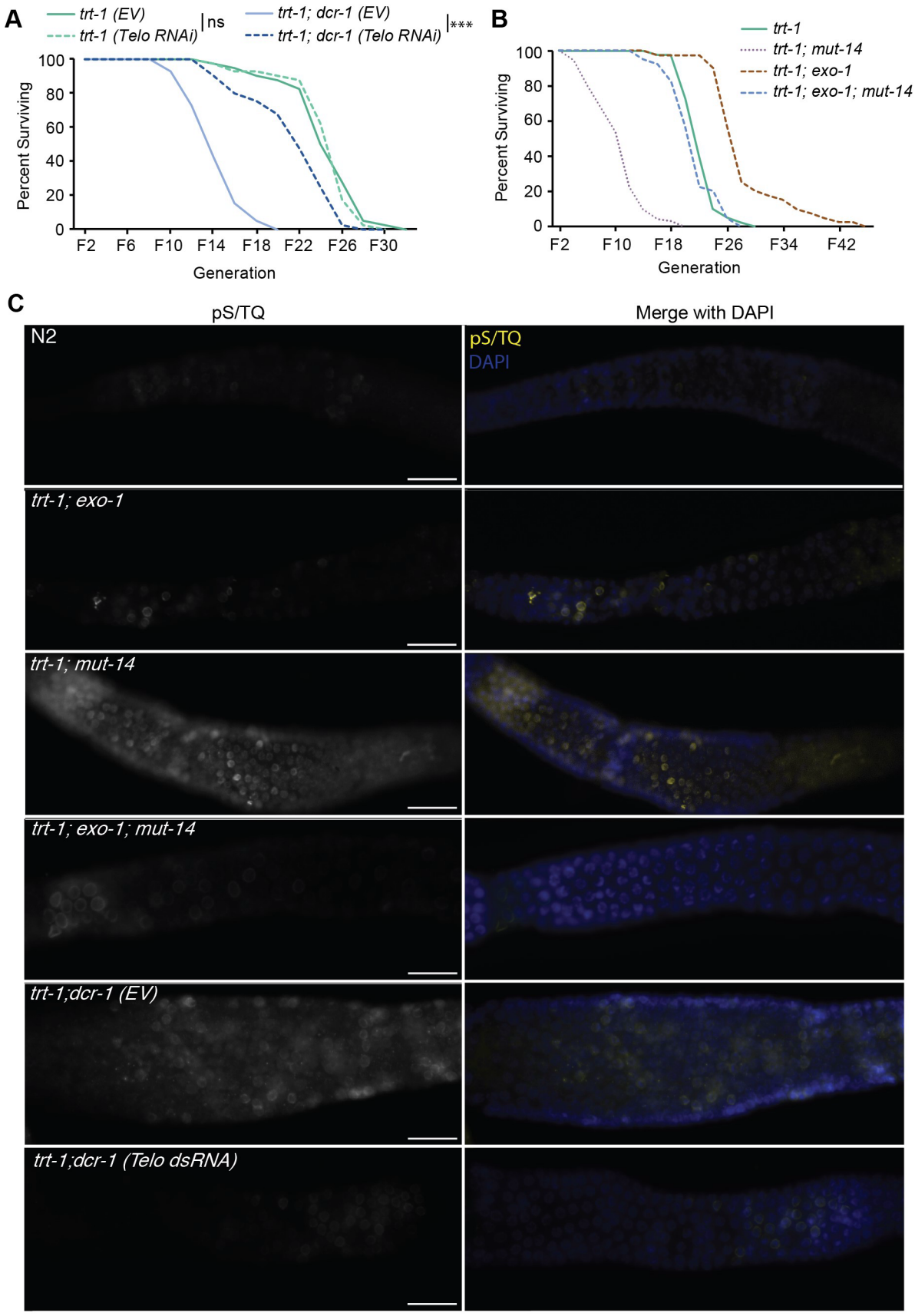
A
trt-1 (EV)
trt-1 (Telo RNAi)
ns
trt-1; dcr-1 (EV)
trt-1; dcr-1 (Telo RNAi)
***
Percent Surviving
100
80
60
40
20
0
F2
F6
F10
F14
F18
F22
F26
F30
Generation
B
trt-1
trt-1; mut-14
trt-1; exo-1
trt-1; exo-1; mut-14
Percent Surviving
100
80
60
40
20
0
F2
F10
F18
F26
F34
F42
Generation
C
pS/TQ
Merge with DAPI
N2
pS/TQ
DAPI
trt-1; exo-1
trt-1; mut-14
trt-1; exo-1; mut-14
trt-1;dcr-1 (EV)
trt-1;dcr-1 (Telo dsRNA)

1094

1095
1096 **Figure 5:** Fast senescence in sRNA-deficient *trt-1* is rescued by exogenous telomeric
1097 dsRNA or loss of Exonuclease-1. (A) Survival of *trt-1* or *trt-1; dcr-1(mg375)* on either
1098 empty vector control (EV) or bacteria expressing telomeric double-stranded RNA (telo
1099 dsRNA). Log rank test relative to EV, ***P < 0.001. n=40 lines per genotype. (B) Loss of
1100 *exo-1* extends survival of *trt-1; mut-14* lines. n=40 lines per genotype. (C) Telomeric
1101 dsRNA and loss of *exo-1* suppress accumulation of phospho-(Ser/Thr) in sRNAdeficient
1102 *trt-1* by F6. Scale bar=20um.
1103
1104

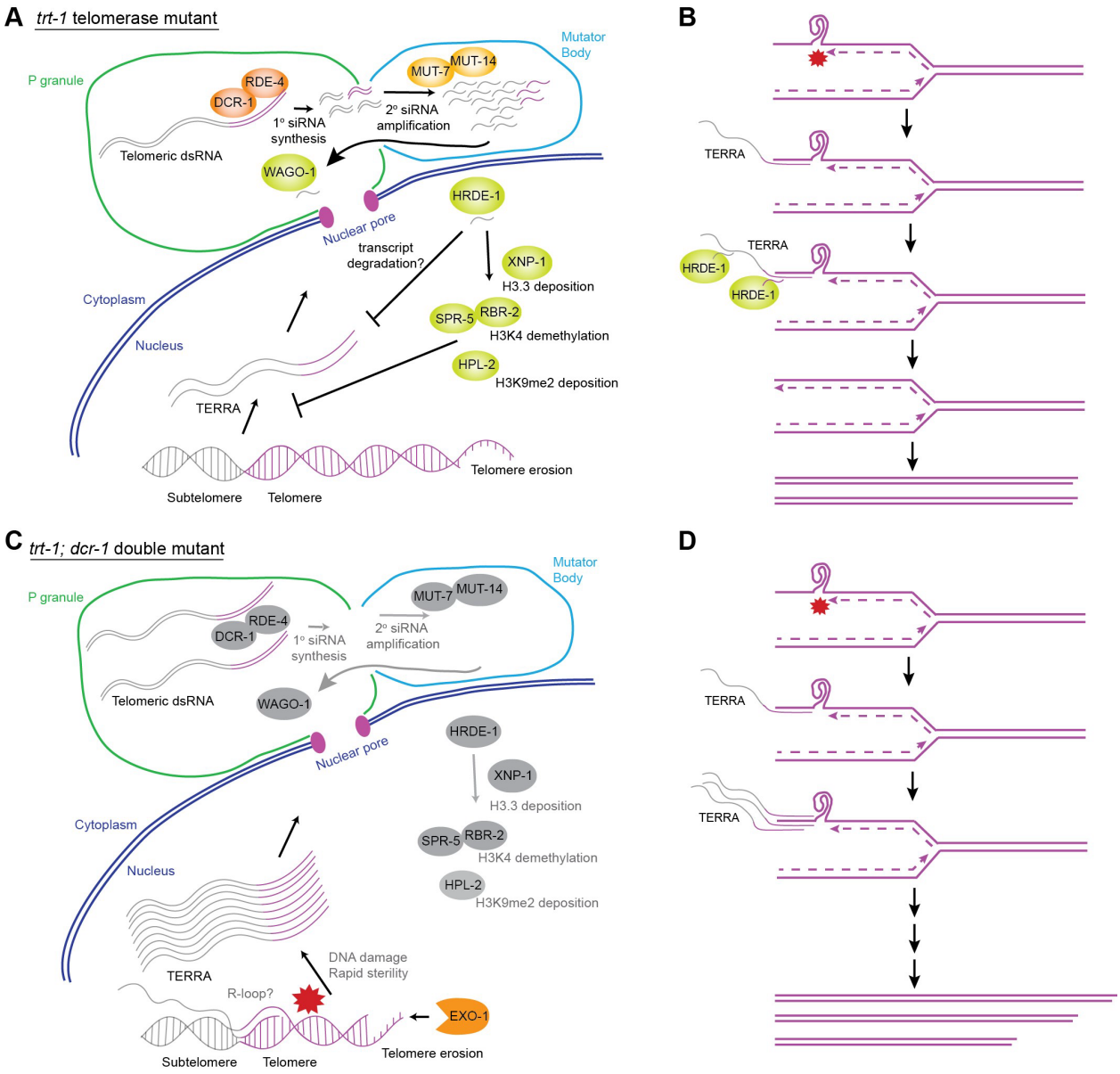


**Figure 6:** Model for TERRA, small RNAs and telomerase. A) In *trt-1* telomerase mutants, telomeric erosion induces expression of the lncRNA TERRA, which engages production of sub-telomeric and telomeric sRNAs. Small RNAs promote deposition of H3K9me2 and H3K4 demethylation in order to repress TERRA expression DNA damage, and *trt-1* mutant sterility. B) TERRA expression and silencing may occur in the context of a DNA damage response. C) In *trt-1; dcr-1* double mutants, TERRA expression is not repressed, which may cause RNA:DNA hybrids and a form of recombination that is dependent on the nuclease EXO-1 and leads to rapid sterility. D) Lack of sRNAs may induce an aberrant recombinational response to DNA damage that results in telomere elongation or shortening.

**Supplemental Information**

5 Supplemental Figures

3 Supplemental Tables

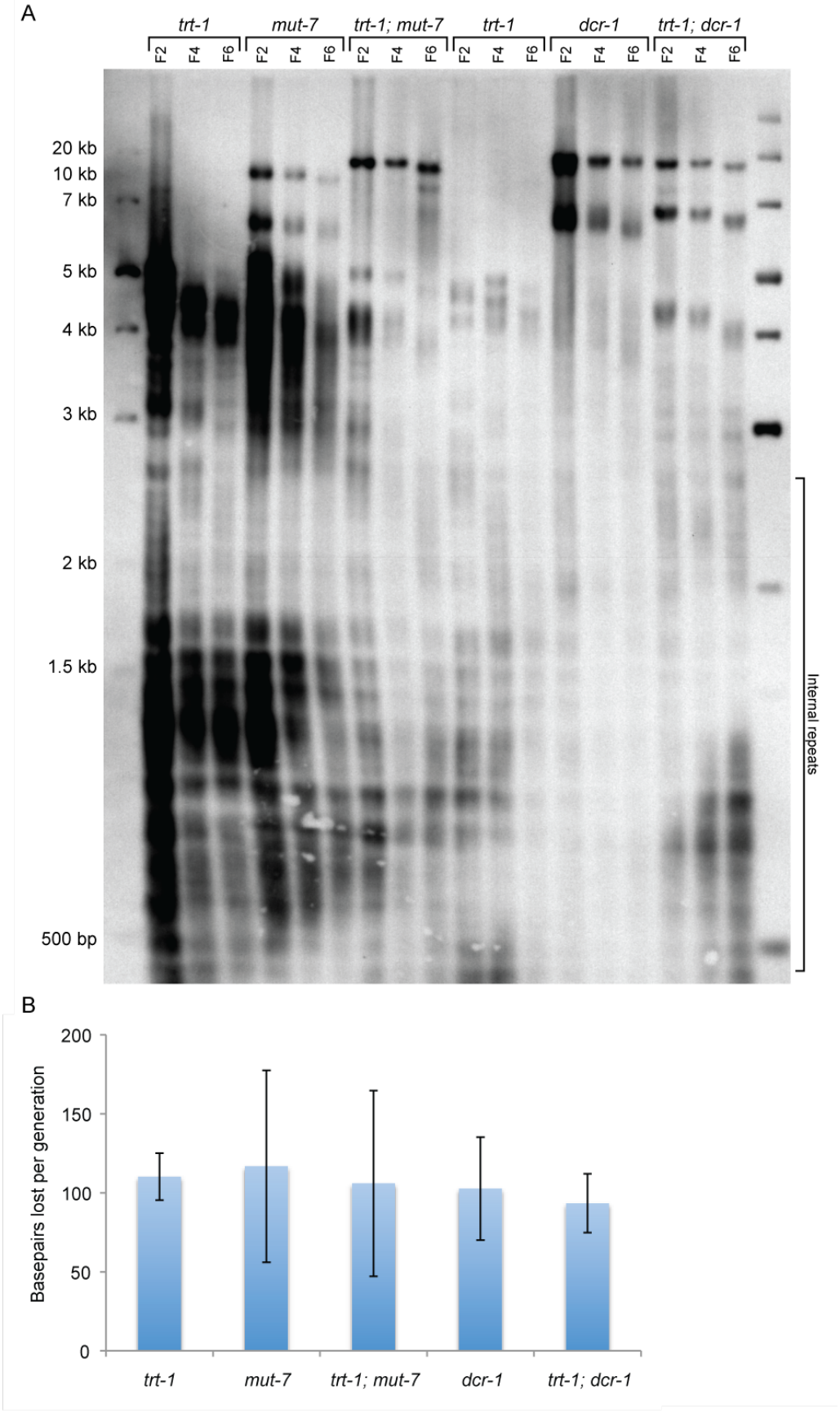
A
trt-1
mut-7
trt-1; mut-7
trt-1
dcr-1
trt-1; dcr-1
F2
F4
F6
20 kb
10 kb
7 kb
5 kb
4 kb
3 kb
2 kb
1.5 kb
500 bp
Internal repeats
B
Basepairs lost per generation
200
150
100
50
0
trt-1
mut-7
trt-1; mut-7
dcr-1
trt-1; dcr-1

1128

1129 **Figure S1. Related to Figure 1.** Terminal Restriction Fragment (TFR) analysis of
1130 single-mutant *trt-1*, *mut-7*, and *dcr-1* and double-mutant *trt-1; mut-7* and *trt-1; dcr-1*
1131 strains using a telomeric probe. (A) Southern blot of samples generated by passaging
1132 small groups of worms for multiple generations. Two independent *trt-1* lines were used.
1133 Long telomeres observed in strains derived from *mut-7* or *dcr-1* mutant background
1134 could be due to rare stochastic telomere elongation events in these backgrounds. (B)
1135 Quantification of telomere shortening rate for each genotype shown in panel A. No
1136 significant difference was found between any genotypes by Mann Whitney U test.
1137

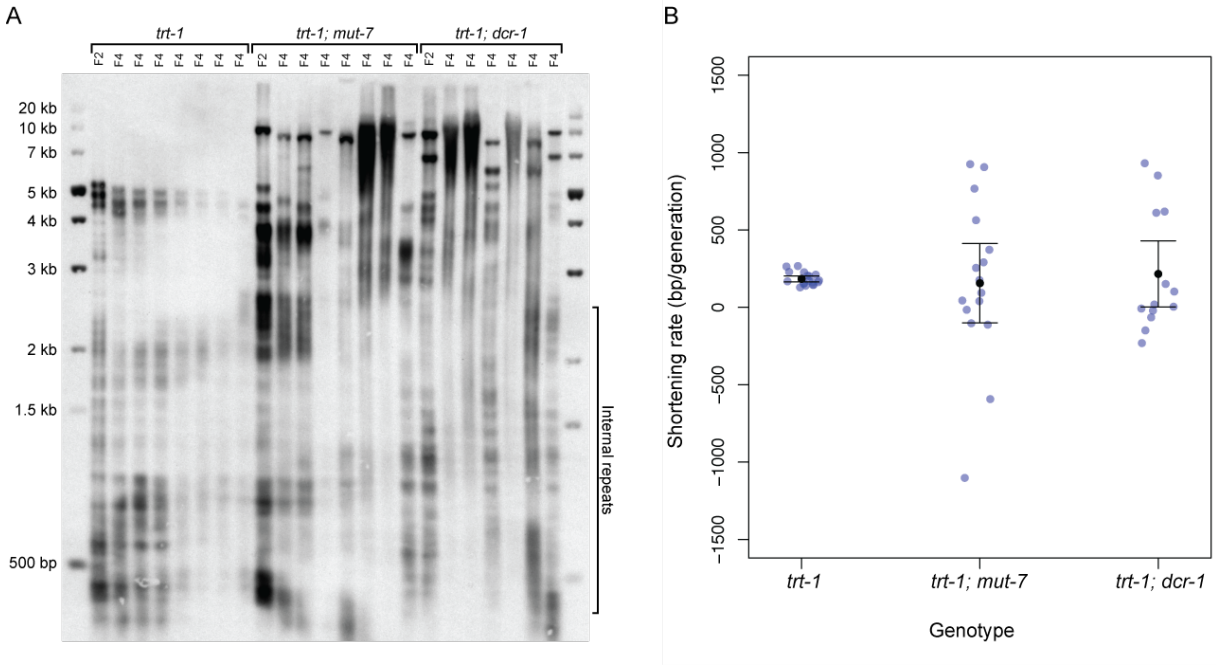


**Figure S2. Related to Figure 1.** TRF analysis of RNAi-deficient telomerase mutant strains using telomeric probe. A) A single parental F2 plate was used to generate multiple F4 plates derived from single worms. F4 *trt-1* single mutant lanes show consistent bands corresponding to slight shortening of parental bands. In contrast, F4 lanes from *trt-1; mut-7* and *trt-1; dcr-1* show highly variable bands that in some cases cannot be traced to an obvious parental band. B) Quantification of telomere shortening rate based on pairing bands appearing at F2 with the closest bands appearing at F4. Highly smeared lanes were excluded. Each point represents one pair of bands. Comparing *trt-1* and *trt-1; mut-7* or *trt-1; dcr-1*, mean shortening rate was not significantly different (p= 0.84 and 0.77, Welch's t-test) but variance was significantly higher for both double-mutants (p=7.2e-15 and 1.5e-12, F-test). Variance was not significantly different between the double-mutants (p=0.32).

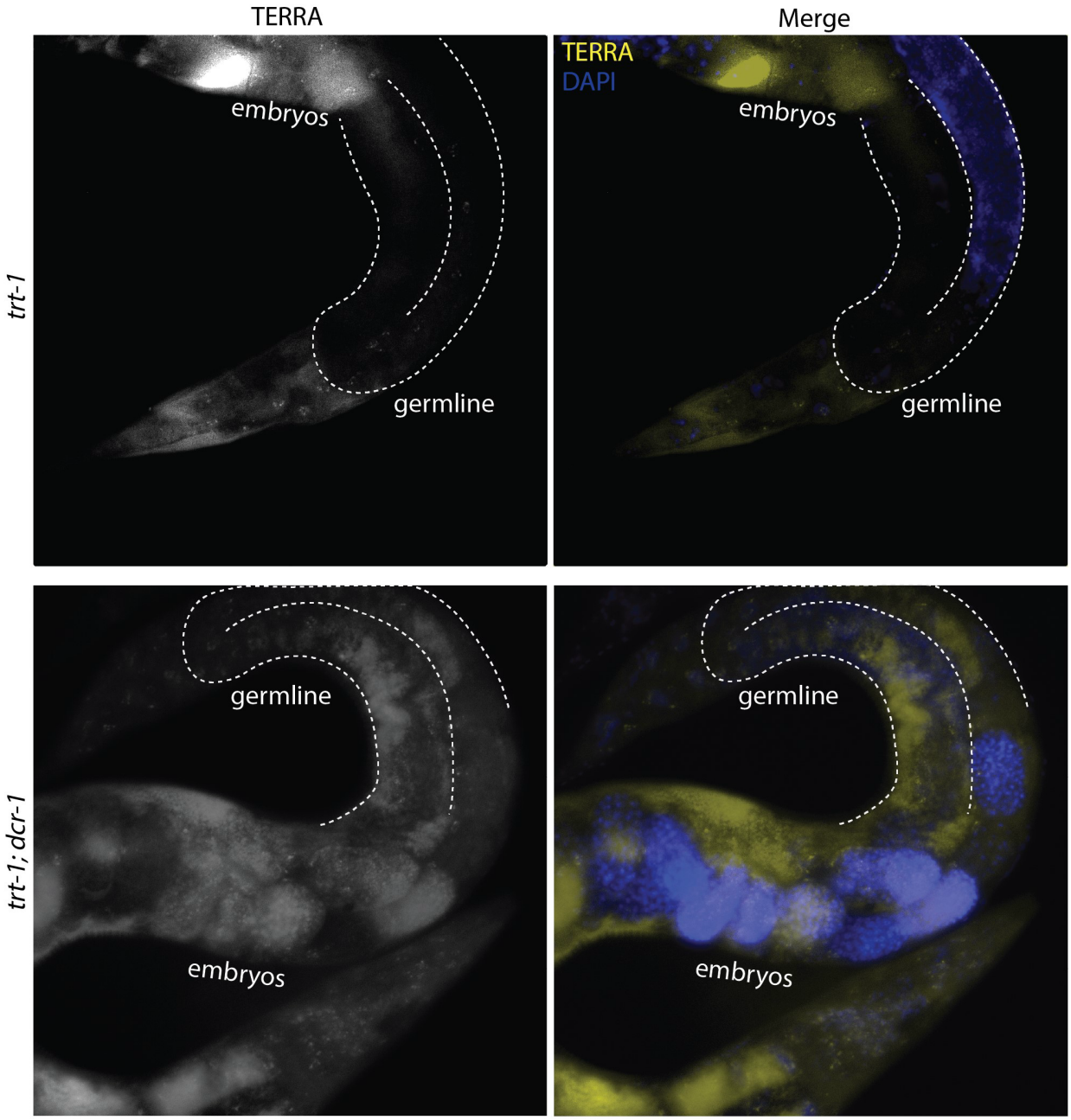


1152

1153 **Figure S3. Related to Figure 2.** TERRA expression (yellow) in *trt-1* and *trt-1;*
1154 *dcr1(mg375)* 1-day-old adults detected with a Cy5-labelled telomeric probe.
1155
1156

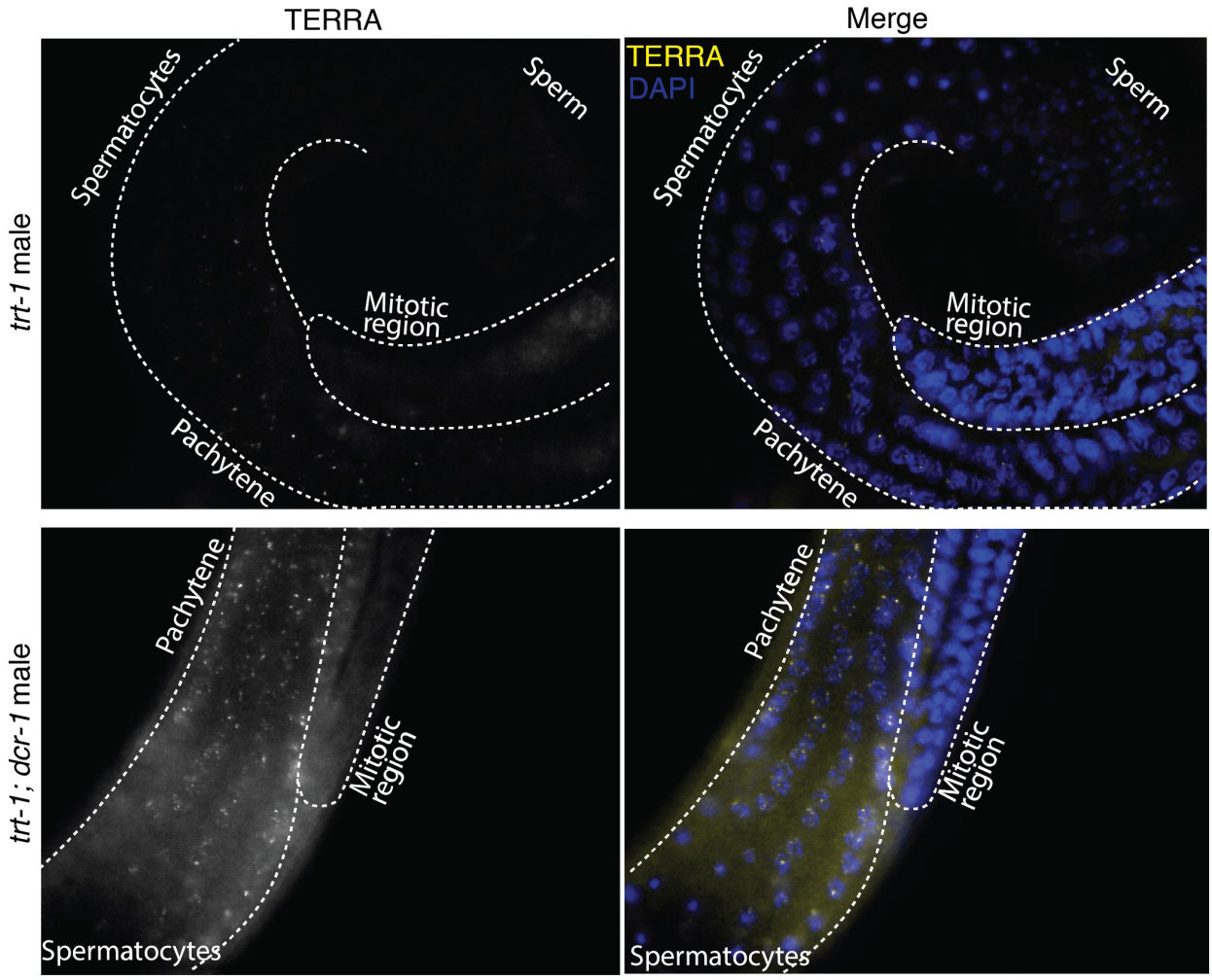


**Figure S4. Related to Figure 2.** RNA FISH of TERRA expression in *trt-1* and *trt-1; dcr1* males. Note TERRA foci in the Pachytene region in both *trt-1* and *trt-1; dcr-1*, as well as lack of expression in the mitotic region and spermatocytes

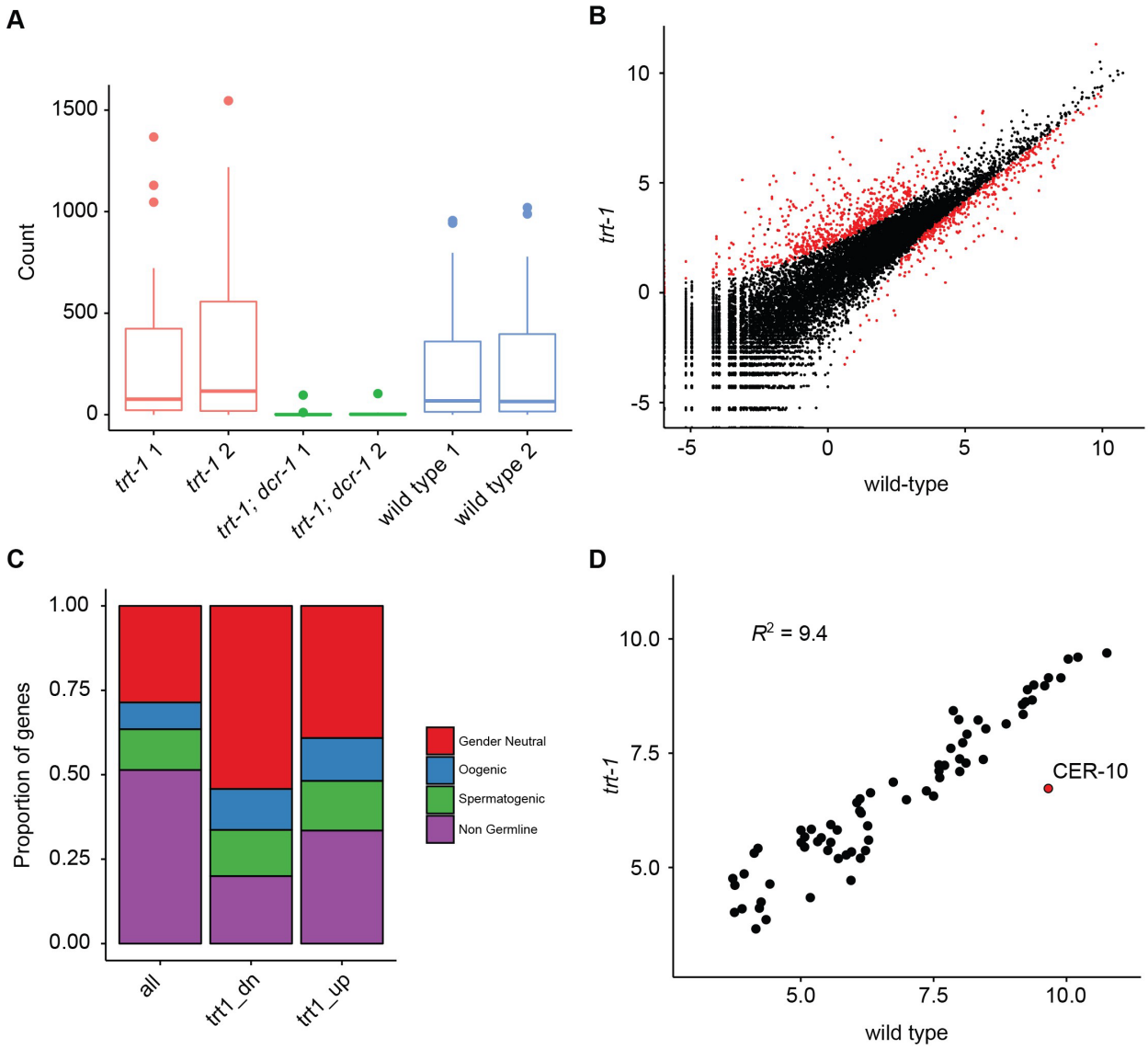


**Figure S5. Related to Figure 3.** Analysis of 22G small RNA species in telomerase and Dicer mutants. (A) Number of reads mapping to DCR-1 targets identified by Gent *et al.* (Gent et al., 2010). (B) log2 normalized mean read counts at every *C. elegans* gene for *trt-1* and wildtype. Genes identified as significantly differentially expressed by DESeq2 are shown in red. ( C) Proportion of all genes or genes downregulated (trt1_dn) or upregulated (trt1_up) belonging to expression categories defined by Ortiz *et al.* (see reference 54 in main text). (D) log2 normalized mean read counts at transposon consensus sequences for *trt-1* and wildtype.

| | Lines tested | Number ALT survivors | Z score | p-value (two tailed) |
|---|---|---|---|---|
| *trt-1* | 40 | 6 | | |
| *trt-1; mut-7(pk204)* | 40 | 4 | 0.68 | 0.50 |
| *trt-1; mut-14(pk738)* | 40 | 4 | 0.68 | 0.50 |
| *trt-1 xnp-1(ok1823)* | 40 | 6 | 0 | 1 |
| *trt-1 xnp-1(tm678)* | 40 | 4 | 0.68 | 0.50 |
| *trt-1; dcr-1 (mg375)* | 40 | 5 | 0.32 | 0.75 |

1195 **Supplemental Table S1. Related to Figure 1.** Statistical analysis of ALT survival in
1196 double mutant strains compared to single mutant *trt-1* control. The Z score represents
1197 how many standard deviations from the number of ALT survivors in double mutants is
1198 from the *trt-1* single mutant control mean survival rate. The p-value represents the
1199 probability that the number of survivors via ALT is not significantly different from the
1200 control *trt-1* single mutant strain.
1201
1202

1213

| Strain | Log Rank test (Z=) | p-value |
|---|---|---|
| *trt-1; mut-7(pk204)* | 9.79 | <0.00001 |
| *trt-1; mut-14(pk738)* | 9.96 | <0.00001 |
| *trt-1; dcr-1(mg375)* | 9.37 | <0.00001 |
| *trt-1; rde-1* | 8.23 | <0.00001 |
| *trt-1; rde-4* | 9.21 | <0.00001 |
| *trt-1; rrf-3* | 8.4 | <0.00001 |
| *trt-1; rrf-2* | 1.7 | 0.089 |
| *trt-1; exo-1* | 7.38 | <0.00001 |
| *trt-1 xnp-1(ok1823)* | 4.3 | <0.00001 |
| *trt-1 xnp-1(tm678)* | 4.23 | <0.0001 |
| *trt-1 xnp-1(tm678); mut-7* | 9.21 | <0.00001 |
| *trt-1; sid-1* | 6.52 | <0.00001 |
| *trt-1; rbr-2(tm1231)* | 8.64 | <0.00001 |
| *trt-1; spr-5 (by101)* | 8.89 | <0.00001 |

1214

1215 **Supplemental Table S2. Related to Figure 1.** Log rank analysis of survival curves of
1216 double or triple mutants compare to single mutant *trt-1* controls. n=40 independent lines
1217 for each genotype. Strains were passaged by transferring 6 larval L1s weekly and scored
1218 as sterile when plates contained no new L1 larvae. The p-value represents the probability
1219 that there is no difference in the probability of sterility at any time point between the
1220 double or triple mutant strain and the *trt-1* single mutant strain.

| *trt-1* F1 | males | dead embryos | *trt-1; dcr-1* F1 | males | dead embryos |
|---|---|---|---|---|---|
| A1 | 13 | 6 | A1 | 0 | 0 |
| A2 | 4 | 26 | A2 | 0 | 0 |
| A3 | 8 | 24 | A3 | 1 | 0 |
| D1 | 10 | 11 | A4 | 0 | 0 |
| D2 | 11 | 4 | B1 | 0 | 0 |
| D3 | 4 | 9 | B2 | 0 | 0 |
| D4 | 13 | 15 | B3 | 0 | 0 |
| | | | B4 | 0 | 0 |
| | | | C1 | 0 | 0 |
| | | | C2 | 0 | 6 |
| | | | C3 | 1 | 0 |
| | | | C4 | 0 | 0 |
| | | | D1 | 0 | 0 |
| | | | D2 | 0 | 0 |
| | | | D3 | 0 | 0 |
| | | | D4 | 0 | 0 |

**Supplemental Table S3. Related to Figure 1.** Counts of total F2 males and dead embryos scored for F1 progeny from crosses of wild-type males with either lategeneration F16 *trt-1* mutant controls (n=2 independently grown strains, three F1 scored for strain A and four F1 for strain D) or early generation F4 *trt-1; dcr-1* double mutant (n=4 strains, 4 F1 each scored for strains A, B, C, and D) hermaphrodites. If a chromosome fusion is present in any of the F1 animals, then it will cause weak nondisjunction of the fused chromosomes, which leads to F2 dead embryos if an autosome is fused or to F2 males if the X chromosome is fused.